



Cite this: *RSC Adv.*, 2025, **15**, 44272

Received 28th July 2025  
 Accepted 5th November 2025

DOI: 10.1039/d5ra05453b

rsc.li/rsc-advances

## Tea-derived catalysts: a sustainable approach to organic transformations

Mohadeseh Amiri, Zahra Vazehi, Masoumeh Abedini\* and Farhad Shirini \*

The increasing demand for sustainable and environmentally friendly catalytic systems has led researchers to use natural resources to develop catalysts. In this line, tea, as a widely consumed beverage rich in bioactive compounds such as polyphenols, has been proposed as an effective material for the synthesis of tea-derived catalysts. These catalysts with unique properties such as high stability, reusability, and improved catalytic activities have been successfully employed in various organic reactions such as reduction, two-component catalytic reactions, multicomponent reactions, and miscellaneous reactions offering high yields under mild and environmentally friendly conditions. This review article explores the preparation, characterization, and application of these types of catalysts, highlighting their potential in transforming organic reactions based on green chemistry rules and advancing sustainable synthetic methods.

### Introduction

The development of sustainable and environmentally benign catalytic systems has become a central theme in modern organic synthesis, driven by the urgent need to reduce reliance on toxic solvents, hazardous reagents, and energy-intensive processes. Among the diverse approaches toward greener catalysis, the utilization of biogenic, biomass-derived, and plant-based catalysts has attracted significant attention due to

their inherent renewability, low cost, and ability to mediate diverse organic transformations under mild conditions. Plant extracts, rich in polyphenols, flavonoids, alkaloids, and terpenoids, provide an eco-friendly reservoir of reducing and stabilizing agents that can facilitate the synthesis of nanomaterials and catalytic systems with enhanced activity and recyclability. These bio-derived systems offer not only a sustainable route for catalyst production but also align with the broader principles of green chemistry and circular economy by minimizing waste and valorizing natural resources.<sup>1-4</sup>

Tea is one of the most widely consumed beverages worldwide, characterized by its bitter and astringent taste, and

*Department of Organic Chemistry, Faculty of Chemistry, University of Guilan, Rasht, 41335-19141, Iran. E-mail: shirini@guilan.ac.ir; mabedini@guilan.ac.ir; Fax: +98 131 3233262; Tel: +981313233262*



**Mohadeseh Amiri**

*Mohadeseh Amiri was born in Tonekabon/Mazandaran, Iran, in 1998. She completed her BSc in Applied Chemistry at the University of Isfahan in 2022. She received her MSc in Organic Chemistry from the University of Guilan under the guidance of Prof. F. Shirini in 2024. Her research interests focus on green chemistry and pharmaceutical synthesis. She plans to pursue a PhD to further advance her research in these areas.*



**Zahra Vazehi**

*Zahra Vazehi was born in Mashhad, Iran, in 1999. She completed her BSc in Pure Chemistry from Shahrood University of Technology in 2022. She received her MSc in Organic Chemistry from the University of Guilan under the guidance of Prof. F. Shirini in 2024. She is currently pursuing her PhD degree in the Department of Chemistry at Isfahan University, Isfahan, Iran. Her current research interests include the preparation of new catalysts and their applications in multicomponent reactions, the preparation of hydrogels and their applications, as well as green chemistry and related sustainable processes.*



produced from the leaves of the *Camellia sinensis* plant. The main types of tea derived from *Camellia sinensis* include:<sup>5,6</sup>

1. Green tea.
2. Black tea.
3. White tea.

Tea infusions (or tisane) are beverages prepared by brewing parts of plants unrelated to *Camellia sinensis*.<sup>7</sup> Some of the most commonly used teas are:<sup>8</sup>

1. Hibiscus tea (*Hibiscus sabdariffa*) – red tea or sour tea.
2. Fenugreek tea (*Trigonella foenum-graecum*).
3. Herbal tea extract (*Stachys lavandulifolia*).
4. Yerba Mate (*Ilex paraguariensis*).

While *Camellia sinensis* teas contain bioactive compounds such as epigallocatechin gallate (EGCG), epicatechin gallate (ECG), and theaflavin, which are well known for their antioxidant, anti-inflammatory, and antimicrobial activities, other herbal infusions also contain a variety of structurally diverse phytochemicals with significant biological activities.<sup>9–12</sup> For instance, *Hibiscus sabdariffa* is rich in delphinidin-3-sambubioside, cyanidin-3-sambubioside, and chlorogenic acid, while *Stachys lavandulifolia* provides apigenin, luteolin, and rosmarinic acid.<sup>13–15</sup> Similarly, *Trigonella foenum-graecum* (fenugreek) contains diosgenin, trigonelline, and 4-hydroxyisoleucine, and *Ilex paraguariensis* (Yerba Mate) is an important source of caffeic acid, chlorogenic acid, and theobromine.<sup>16–18</sup> The chemical structures of these compounds are shown in Fig. 1, while the biogenic synthesis of chlorogenic acid from glucose is schematically illustrated in Fig. 2.<sup>19</sup> These diverse phytochemicals serve as natural reducing and stabilizing agents in nanocatalyst preparation, providing renewable, eco-friendly, and cost-effective alternatives to conventional synthetic methods.<sup>20,21</sup>

Moreover, many tea derivatives are not only valuable sources of bioactive compounds but also serve as suitable substrates and reaction media for the preparation of novel catalytic

systems. Such catalysts can be efficiently designed and applied as recoverable promoters in a variety of organic transformations, including reduction, Suzuki coupling, two-component, three-component, and other organic reactions. The prepared systems demonstrate remarkable catalytic efficiency, allowing reactions to proceed with good to high yields within short, acceptable reaction times. This article provides a concise review of these developments, emphasizing the role of tea-derived compounds in the design of sustainable and effective catalytic systems.<sup>22,23</sup>

### Biogenic nanoparticles and the role of plant materials in their preparation

Biogenic nanoparticles represent an emerging class of catalytic materials prepared using plant-derived metabolites as reducing and capping agents. Unlike conventional chemical synthesis, which often requires high temperatures, toxic solvents, and hazardous reducing agents, biogenic synthesis is typically conducted under mild, aqueous conditions, generating nanoparticles with controlled morphology and stability.<sup>24</sup> Plant metabolites such as polyphenols, flavonoids, and alkaloids promote nucleation and growth of nanoparticles, while simultaneously preventing aggregation through surface passivation. This dual role enables the formation of highly stable and catalytically active nanostructures.<sup>25–27</sup>

The use of plant extracts in nanoparticle synthesis provides several advantages: (i) simplicity and cost-effectiveness, since no additional stabilizing ligands are needed; (ii) alignment with green chemistry by reducing waste and eliminating toxic reagents; and (iii) tunability, as the diversity of phytochemicals across different plant species leads to nanoparticles with distinct physicochemical properties.<sup>28–30</sup> For instance, extracts from *Hibiscus sabdariffa* have been employed for the green synthesis of zinc oxide and copper oxide nanoparticles, yielding systems with remarkable antibacterial and catalytic



Masoumeh Abedini

the synthesis of new catalysts and their applications in organic synthesis and multi-component reactions.



Farhad Shirini

Farhad Shirini was born in Tehran, Iran, in 1965. He received his MSc in organic chemistry from Shiraz University, under the guidance of Professor N. Iranpoor in 1990. He started his doctoral work under the supervision of Professor H. Firouzabadi in Shiraz University and obtained his PhD degree in 1995. He has been a faculty member of the University of Guilan since 1995. His current research interests include development of new synthetic methodologies using both homogeneous and heterogeneous catalysts, multi-component reactions, and synthesis of new catalysts such as *N*-sulfonic acids, nano catalysts and ionic liquids and application of these catalysts in various reactions.



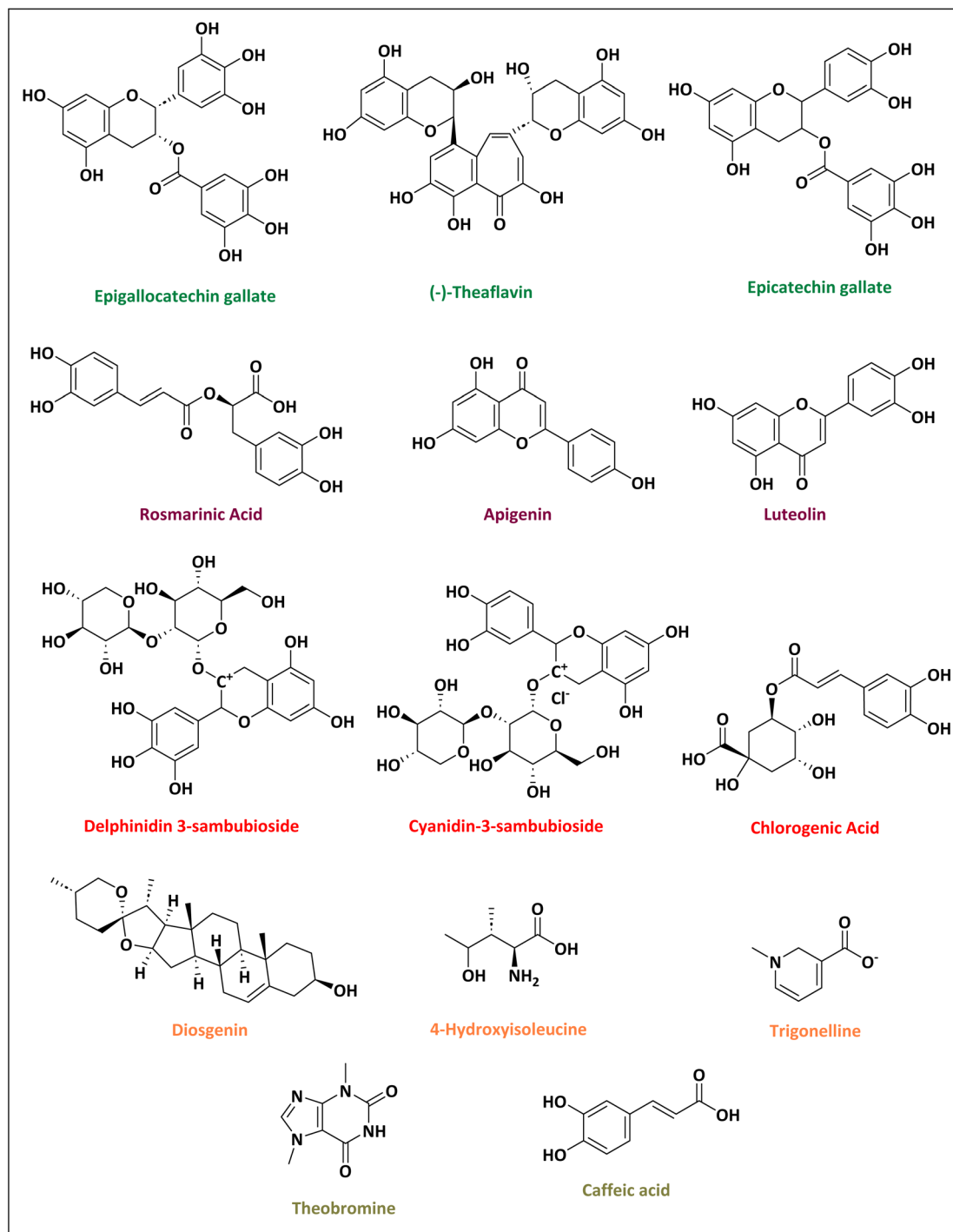


Fig. 1 Chemical structures of some important natural compounds present in the teas studied.

activities.<sup>31,32</sup> Similarly, *Rhododendron arboreum* extract has been used to generate magnetically recoverable  $\text{Fe}_3\text{O}_4$  nanoparticles exhibiting excellent recyclability in nitroarene reduction.<sup>33</sup>

#### Reduction of nitro aromatics

Nitro aromatics are an important class of organic compounds which in them at least one nitro group ( $-\text{NO}_2$ ) is covalently

attached to a carbon atom of an aromatic ring.<sup>34,35</sup> These compounds are used in the pharmaceutical, dyeing, wood preservatives, rubber making, pesticide and explosive industries.<sup>36–38</sup> Despite their wide-ranging applications, most nitroaromatics are toxic, carcinogenic, and environmentally persistent, and are commonly found in industrial effluents, where their release into water sources causes serious environmental problems.<sup>38,39</sup>

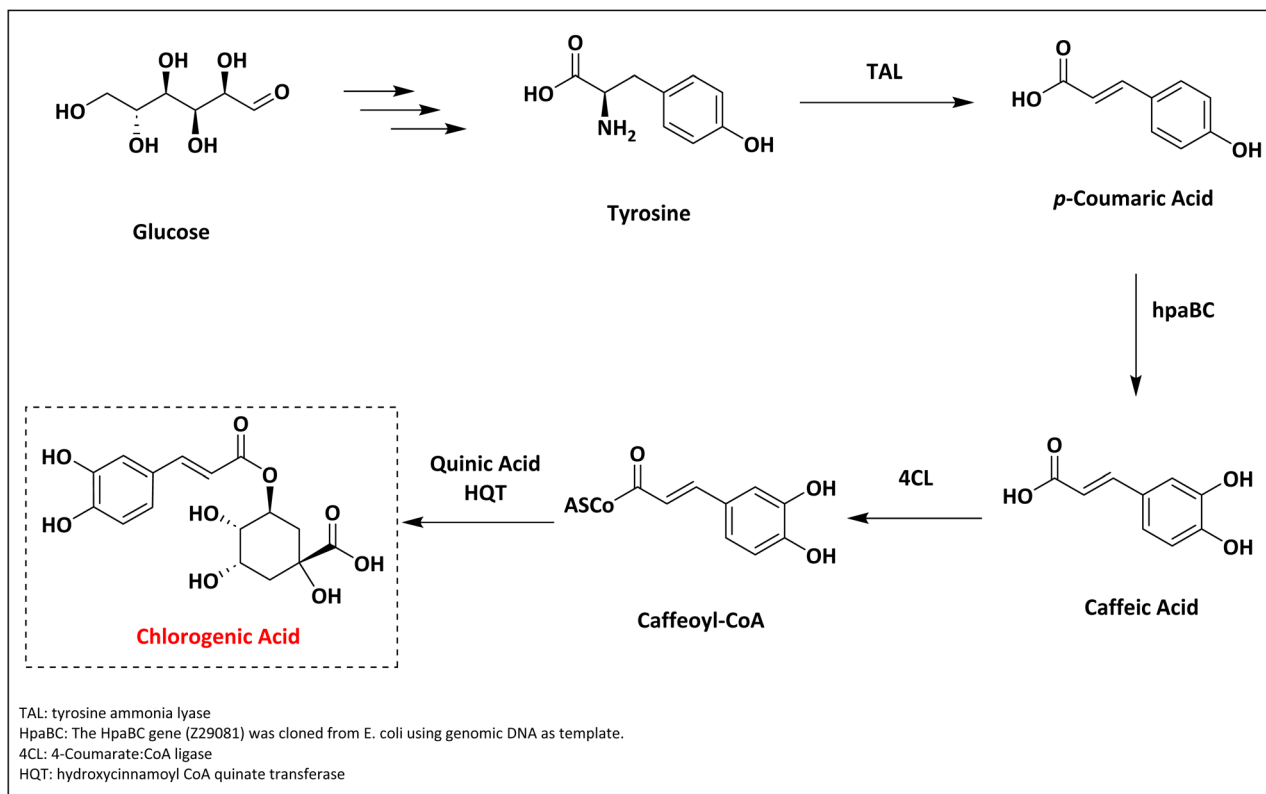


Fig. 2 Biogenic synthesis of chlorogenic acid from glucose.

Various methods have been developed to remove these harmful compounds from industrial wastewater, including: absorption, coagulation, electrocoagulation,<sup>40</sup> reverse osmosis,<sup>41</sup> biological and chemical decomposition,<sup>42</sup> catalytic oxidation under microwave,<sup>43</sup> electrofenton,<sup>44</sup> and photocatalytic degradation;<sup>45</sup> however, many of these methods face limitations such as low reaction rates and difficulties in finding suitable microorganisms.

In recent years, catalytic hydrogenation of nitroaromatics has attracted significant attention as a green, economical, and energy-efficient approach, effectively converting toxic compounds into useful amines and removing them from the environment.<sup>46–49</sup>

This goal can be reached *via* different ways of them the use of noble metals and sulfuric acid is the common one.<sup>50</sup> Among the disadvantages of this process, we can mention the use of corrosive mineral acid and the high cost of the noble metals used. In recent years, utilizing green chemistry-based methods has greatly developed. Based on this, the path of catalytic reduction of nitrophenols to aminophenols in aqueous environments under mild conditions has been widely studied.<sup>51,52</sup>

In this line, biogenically prepared catalysts, using plant extracts such as hibiscus tea, green tea, black tea and fenugreek tea offer significant advantages over traditional systems. These extracts simultaneously function as green reducing agents and stabilizing/capping agents. Polyphenols, flavonoids, and hydroxyl groups in the tea extracts reduce metal ions ( $\text{Ag}^+$ ,  $\text{Pd}^{2+}$ ,

$\text{Au}^{3+}$ ) to zero-valent nanoparticles ( $\text{Ag}^0$ ,  $\text{Pd}^0$ ,  $\text{Au}^0$ ) and initiate catalytic activity, while the biological compounds in the extracts form a protective layer that prevents nanoparticles aggregation and maintains high dispersibility and stability of the catalyst. This dual functionality eliminates the need for hazardous chemical reducing or stabilizing agents, making the process fully compatible with green chemistry principles.<sup>53–55</sup>

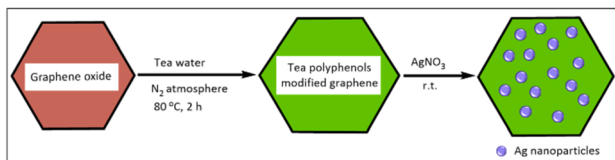
Overall, in green nitro group reduction reactions, the use of biogenic catalysts prepared with plant extracts, which act as reducing and stabilizing agents, offers advantages over conventional reagents; these benefits include increased reaction rate, selectivity, and stability while maintaining mild conditions.<sup>56–58</sup> Furthermore, the synthesis of catalysts with green hydrogen sources provides a safe, efficient, and environmentally sustainable strategy for the reduction of nitroaromatics, converting these toxic compounds into valuable amines under controlled and stable conditions, which serve as essential intermediates for the synthesis of pharmaceuticals, dyes, agrochemicals, and other valuable organic compounds.<sup>59</sup>

For this purpose, a variety of catalytic methods have been reported which in them tea-based reagents play key roles.

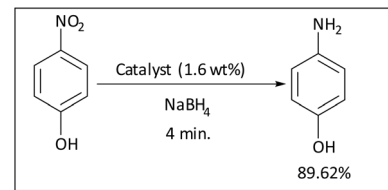
In 2015, Wang and co-workers prepared a water-dispersible Ag-TPG (tea polyphenols modified graphene) nanohybrid catalyst using a facile *in situ* green reduction strategy.<sup>60</sup>

The requested catalyst was prepared by knowing that polyphenolic compounds extracted from green tea can effectively reduce graphene oxide (GO) and adsorb on the surface of it. In continue, by adding  $\text{AgNO}_3$ , the surface adsorbed tea

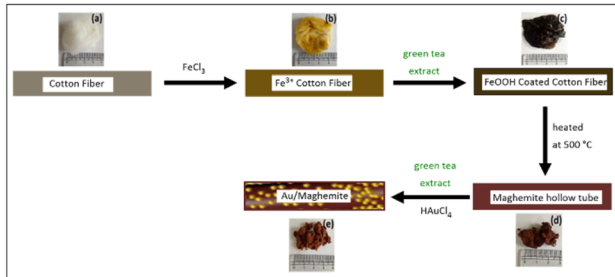




**Scheme 1** Green reduction process of graphene oxide followed by *in situ* reduction of silver ions to form Ag-TPG nanohybrid.



**Scheme 3** Reduction of 4-nitrophenol to 4-aminophenol mediated by the catalyst.



**Scheme 2** Step-by-step synthesis of hierarchical magnetic tubes decorated with gold nanoparticles with physical appearance (scale in centimeters).

polyphenols can reduce Ag ions to silver nanoparticles *in situ* and stabilize them (Scheme 1).

In this research, UV-vis and FT-IR analyses revealed that tea polyphenols contributed to the reduction and stabilization of graphene while preserving surface oxygen groups. XPS and TGA further confirmed the stable presence of polyphenols, whereas XRD and TEM evidenced the uniform distribution of Ag nanoparticles (3–5 nm) on the graphene support. Accordingly, the Ag-TPG nanohybrid with a stable structure was employed for the reduction of 4-NP. Therefore, Ag-TPG nanohybrid, which consists a combination of unique catalytic properties of silver nanoparticles and excellent absorption and electron transfer capability of graphene, was employed as a catalytic system for the reduction of 4-nitrophenol (4-NP) by NaBH<sub>4</sub>. In this reaction, a solution of 4-NP (0.1 mM) and NaBH<sub>4</sub> (10 mM) after removing oxygen with nitrogen gas, was combined with a suspension of Ag-TPG (0.5 mg mL<sup>-1</sup>) purged with nitrogen under magnetic stirring conditions. The reaction proceeded for 12 min with 100% conversion. The recycled Ag-TPG catalyst showed similar catalytic behavior compared to the fresh one even after five times of recycling, indicating the considerable stability of the Ag-TPG catalyst under the applied conditions.

In 2018, Purbia and co-worker proposed a new, efficient, and stable synthetic method for the preparation of hierarchical magnetic maghemite catalyst ( $\gamma$ -Fe<sub>2</sub>O<sub>3</sub>) accompanied by Au nanoparticles (NPs).<sup>55</sup>

In this study, firstly the cotton sample was soaked in the FeCl<sub>3</sub> solution and subjected to ultrasound, and then it was immersed in the green tea leaf extract; this initial step facilitated the uniform adsorption of iron ions onto the cotton fibers and was critical for the formation of iron oxide tubular structures. The polyphenols present in green tea provide a mild and

environmentally friendly coordination environment for Fe<sup>3+</sup> ions, ensuring their homogeneous distribution on the cotton fibers while maintaining a completely green process. To produce iron oxide micro/nanotubes, the sample was heated at 500 °C in a muffle furnace to separate the cotton fibers. The resulting tubular structures were then dispersed in ultrapure water to eliminate chloride ions and were isolated using an external magnetic field. Then HAuCl<sub>4</sub> solution was introduced into the suspension of iron oxide tubes under ultrasonic conditions. Finally, green tea extract was employed as a reducing agent to obtain iron oxide tubes decorated with gold. Similarly, tubes decorated with other noble metals, such as Ag and Pd, were synthesized using their corresponding metal precursors, including AgNO<sub>3</sub> and Na<sub>2</sub>PdCl<sub>4</sub> (Scheme 2).

FT-IR and XPS confirmed that green tea polyphenols acted as reducing and stabilizing agents, converting Fe<sup>3+</sup> to Fe<sup>2+</sup> and maintaining surface functionalities. XRD, UV-Vis, TEM, FE-SEM, and BET showed well-crystallized  $\gamma$ -Fe<sub>2</sub>O<sub>3</sub> tubes with uniform Au nanoparticles (7 ± 2 nm) and high surface area, highlighting the essential role of tea in formation, stabilization, and catalytic activity of the nanocomposite.

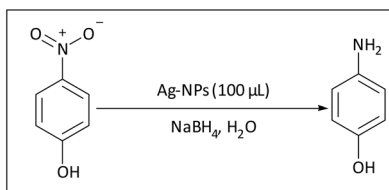
After characterization the synthesized catalyst showed excellent activity in the reduction of 4-nitrophenol to 4-aminophenol (Scheme 3). The reduction reaction of 4-NP was carried out with NaBH<sub>4</sub> (80 mM) in the presence of the maghemite tubes containing 1.6 wt% of Au NPs, achieving a conversion of 89.62%. The reusability of the catalyst was also investigated and only 0.29% of its activity decreased after the sixth cycle. In addition, silver and palladium nanoparticles decorated with  $\gamma$ -Fe<sub>2</sub>O<sub>3</sub> tubes were also synthesized and tested for the same catalytic reaction. The results showed highest activity for palladium.

In 2017, silver nanoparticles were prepared using the *Hibiscus sabdariffa* leaf (roselle or sour tea) by Kalita and co-worker.<sup>53</sup>

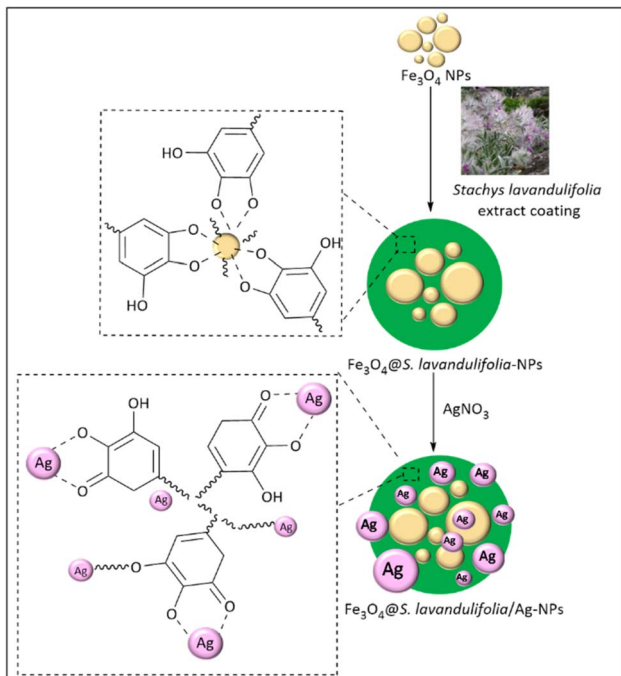
For this purpose the *Hibiscus sabdariffa* leaf extract as a reducing and stabilizing agent was added to an aqueous solution of AgNO<sub>3</sub>. After the reduction of silver ions to the nano silver particles, the colloidal solution was centrifuged. This process was repeated three times to get rid of any unnecessary plant materials.

UV-Vis and TEM showed mostly spherical Ag-NPs (~26.5 nm) with controlled size and shape, while XRD confirmed high crystallinity (13.9 nm). FT-IR indicated phenolic, hydroxyl, and amino groups from hibiscus extract, acting as both reducing and capping agents, highlighting its role in rapid reduction,





**Scheme 4** Catalytic reduction of 4-nitrophenol to 4-aminophenol by  $\text{NaBH}_4$  using Ag-NPs as the catalyst.



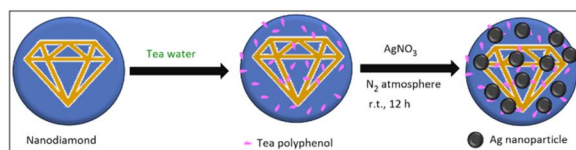
**Scheme 5** Synthetic pathway of  $\text{Fe}_3\text{O}_4@\text{S. } \text{Lavandulifolia}/\text{Ag}$  nanocatalyst.

stabilization, and shape-controlled formation of AgNPs under green chemistry conditions.

In continue the prepared reagent was used as a catalyst in the reduction of 4-nitrophenol with sodium borohydride (Scheme 4). In this experiment, an aqueous solution of 4-nitrophenol was mixed with  $\text{NaBH}_4$ , and the color change from light yellow to yellow-green indicates the formation of 4-nitrophenolate ion.

For the first time, in 2018, Shahriary *et al.* designed an environment-friendly novel hybrid magnetic nanocomposite ( $\text{Fe}_3\text{O}_4@\text{S. } \text{Lavandulifolia}/\text{Ag}$ ) considering the reduction and stabilization potency of metal nanoparticles.<sup>54</sup>

To prepare *Stachys lavandulifolia* extract, freshly collected herbal tea from Kermanshah, Zagros region of Iran was used. After straining, the prepared extract was stored in a refrigerator at 4 °C for further use. In order to synthesis the  $\text{Fe}_3\text{O}_4@\text{S. } \text{Lavandulifolia-NPs}$ , in the first step, magnetite nanoparticles were dispersed in water and subjected to ultrasound for 20 minutes. The herbal tea extract which contains phenolic functional groups which can be used in the modification of Fe<sub>3</sub>O<sub>4</sub>-NPs was added to the mixture. After that, a solution of  $\text{AgNO}_3$  in



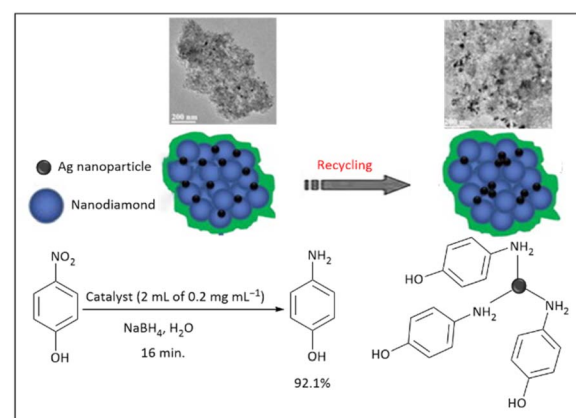
**Scheme 6** Schematic diagram of the Ag-TPND catalyst preparation process.

$\text{H}_2\text{O}$  was added to the obtained product, and then  $\text{Fe}_3\text{O}_4@\text{S. } \text{Lavandulifolia}/\text{Ag-NPs}$  were separated by magnetic discharge (Scheme 5).

FT-IR, XRD, and XPS confirmed the reduction of  $\text{Ag}^+$  to  $\text{Ag}^0$  by the phenolic and flavonoid groups, as reducing and stabilizing agents in *S. lavandulifolia* extract. FESEM, HRTEM, and EDS revealed a uniform biopolymer coating with well-dispersed Ag NPs, while VSM showed slightly reduced magnetization due to the extract coating and Ag loading. After the mentioned studies, the prepared catalyst was used in the reduction of 4-nitrophenol. For the catalytic test of  $\text{Fe}_3\text{O}_4@\text{S. } \text{Lavandulifolia}/\text{Ag-NPs}$ , the reaction was carried out in a quartz cuvette by mixing the freshly prepared solutions of 4-nitrophenol (3 mM) and  $\text{NaBH}_4$  (0.3 M) and adding 2 mg of the catalyst, where complete conversion of 4-NP to 4-AP was achieved. This catalyst was recycled 9 times and no significant decrease in its catalytic activity was observed.

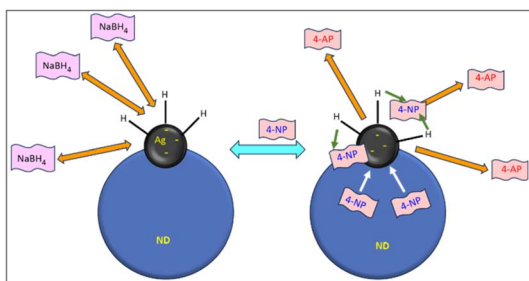
Wang *et al.* reported the preparation of a novel heterogeneous catalyst by modifying the nanodiamond (ND) surface with tea polyphenols (TPs) and subsequent green reduction method to prepare a water-dispersible Ag-TPND hybrid.<sup>61</sup>

For this aim, at first the clear water solution of TPs was obtained by extracting green tea polyphenols through the removal of green tea leaves by centrifuging the filtered solution to completely remove the impurities. Then, ND surface was modified using the newly prepared TPs solution. After the completion of the reaction, the TPND hybrid was acquired by centrifugal separation. In the next step, the prepared TPND powder was sonicated in deionized water and then, the  $\text{AgNO}_3$  solution was added dropwise to it. Finally, by centrifugal separation, the Ag-TPND catalyst was obtained (Scheme 6).



**Scheme 7** Catalytic reduction of 4-nitrophenol to 4-aminophenol in the presence of Ag-TPND.



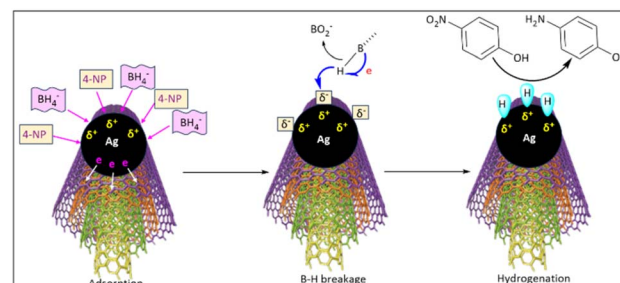


**Scheme 8** Mechanism of the catalyzed reduction of 4-NP to 4-AP by  $\text{NaBH}_4$  in the presence of Ag-TPND.

FT-IR, UV-Vis, XRD, and XPS analysis confirmed that phenolic and hydroxy groups of TPs reduced  $\text{Ag}^+$  to  $\text{Ag}^0$  and stabilized Ag NPs on ND. TEM showed uniform, small Ag NPs (2–10 nm) well-dispersed on ND, while TGA and dispersibility tests indicated a stable TPs coating providing excellent aqueous stability. ICP-AES verified successful Ag loading ( $\sim 0.13\text{--}0.15\%$ ). To evaluate the ability of the Ag-TPND catalyst, the reduction of 4-nitrophenol with  $\text{NaBH}_4$  was carried out in the presence of it in aqueous solution under nitrogen atmosphere with final concentrations of 4-NP (0.1 mM),  $\text{NaBH}_4$  (10 mM) and Ag-TPND ( $0.2\text{ mg mL}^{-1}$ ) in a standard quartz cell (Scheme 7), giving a conversion of 92.1%. Further studies clarified that after five times recycling, the catalyst still had a stable and comparable activity compared with the new catalyst.

The proposed mechanism for the reduction of 4-nitrophenol by  $\text{NaBH}_4$  in the presence of the Ag-TPND catalyst is shown in Scheme 8 based on the Langmuir-Hinshelwood (LH) model.

Veisi and co-workers introduced a new heterogeneous nanocatalyst Ag NPs/MWCNTs@*S. lavandulifolia* in 2019 with



**Scheme 10** Proposed mechanism for the catalytic reduction of 4-NP by  $\text{NaBH}_4$  in the presence of Ag-NPs/MWCNTs@*S. lavandulifolia*.

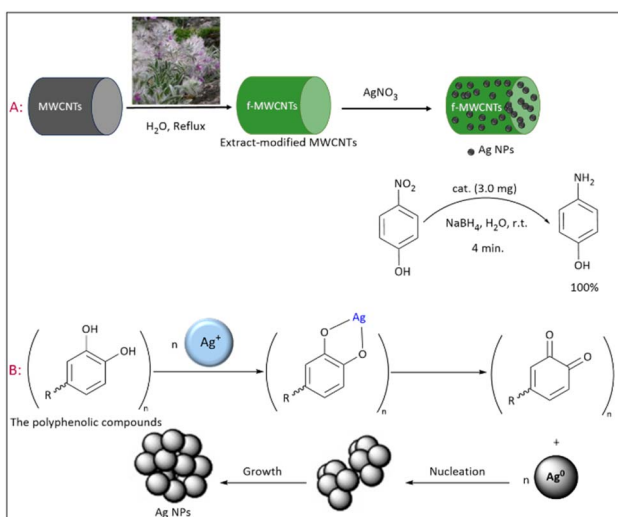
a new green process using *Stachys lavandulifolia* extract as stabilizing and reducing agent.<sup>62</sup>

To prepare the extract of *S. lavandulifolia*, the herbal infusion was collected fresh from Kermanshah, Zagros region of Iran, and after washing, it was added dry to Milli-Q water, and after heating, the extract was filtered with Whatman No. 1 filter paper and mixed. Then, it was centrifuged to remove possible aggregates. In the next step, the mentioned extract was poured into MWCNTs (multi-walled carbon nanotubes) and sonicated. The final deposition of MWCNTs@*S. lavandulifolia* was dispersed in deionized water after centrifugation. Then, by adding  $\text{AgNO}_3$ , it resulted in uniform distribution of Ag-NPs on the surface. Finally, the desired product with the formula of Ag-NPs/MWCNTs@*S. lavandulifolia* was obtained (Scheme 9).

After the preparation, FT-IR, XRD, and XPS confirmed that flavonoids and terpenoids in *S. lavandulifolia* extract reduced  $\text{Ag}^+$  to  $\text{Ag}^0$  and stabilized Ag NPs on MWCNTs. TEM and FE-SEM showed small, uniform, well-dispersed Ag NPs with a biopolymer coating, while EDX and ICP-AES verified the presence of C, O, N from the extract and quantified Ag at  $0.34\text{ mmol g}^{-1}$ , indicating successful coverage, capping, and loading. In continue, Ag-NPs/MWCNTs@*S. lavandulifolia* was used as a nanocatalyst in the reduction of 4-nitrophenol. In this method, the reduction process using  $\text{NaBH}_4$  was carried out in the presence of the catalyst at ambient temperature for 4 min, reaching 100% conversion. The obtained results clarified that coating of silver nanoparticles on carbon nanotubes together with *S. lavandulifolia* extract biopolymer increased the catalytic activity and facilitated the reduction of the nitro group. Also in this study, the catalyst was recovered 7 times without any significant loss of its catalytic activity. A catalytic mechanism is proposed to elucidate the catalytic performance of Ag NPs/MWCNTs@*S. lavandulifolia* as shown in Scheme 10.

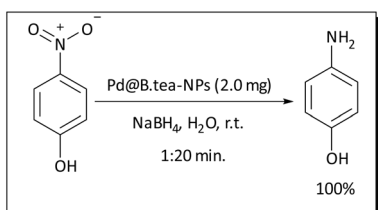
In 2017, an efficient method for the preparation of the Pd@B.tea-NPs catalyst using the natural black tea leaves extract (*Camellia sinensis*) was reported by Lebaschi and co-workers.<sup>63</sup>

To prepare the requested reagent, black tea leaves (*Camellia sinensis*) were obtained from Lahijan Tea Research Center, Lahijan, Iran. After adding deionized water to the selected tea leaves and it's boiling, it was cooled and filtered through Whatman No. 1 filter paper to obtain an aqueous extract. To prepare Pd-NPs, the prepared plant extract was added dropwise to the  $\text{PdCl}_2$  solution and refluxed. The color of the reaction

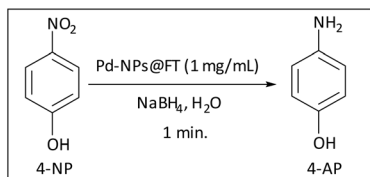


**Scheme 9** (A): Depiction of the eco-friendly functionalization process for MWCNTs, subsequent *in situ* reduction of  $\text{Ag}^+$  ions leading to the formation of Ag-NPs on functionalized MWCNTs (f-MWCNTs) via *Stachys lavandulifolia* extract, producing the Ag NPs/MWCNTs@*S. lavandulifolia* nanocatalyst utilized in 4-nitrophenol reduction; (B): suggested mechanism for Ag-NPs synthesis by *Stachys lavandulifolia* extract.





**Scheme 11** Reduction of 4-nitrophenol in the presence of Pd@B.tea-NPs as the catalyst.



**Scheme 12** Schematic presentation of the reduction of 4-nitrophenol catalyzed by Pd-NPs@FT.

mixture gradually changed, indicating the formation of the Pd nanoparticles, to which acetone was added to precipitate the catalyst (Pd@B.tea-NPs).

Use of the data obtained from UV-Vis, FT-IR, and XRD analysis confirmed  $\text{Pd}^{2+}$  reduction to crystalline  $\text{Pd}^0$  NPs by black tea extract, evidencing the presence of flavonoids, polyphenols, terpenoids, and polysaccharides. TEM, FESEM, EDX, and TGA showed that small (5–8 nm), spherical Pd NPs uniformly coated and stabilized by bio-polymer layers from the extract, preventing aggregation. In continue, the catalytic activity of Pd@B.tea-NPs in the reduction of 4-nitrophenol to 4-aminophenol in water at ambient temperature was investigated. The optimal reaction conditions included the use of 2.0 mg of the catalyst and 250 mM  $\text{NaBH}_4$ , which showed the highest efficiency with 100% conversion. The results showed that Pd@B.tea-NPs has a higher catalytic activity compared to Pd-NPs alone (conversion = 96%), which can be attributed to the presence of the reactive species on the surface of the extract (Scheme 11). The recoverability and reusability of Pd@B.tea-NPs in this reaction was also investigated. It was found that the catalyst maintains its activity during at least nine catalytic cycles in the reduction of 4-NP.

Mallikarjuna *et al.* presented a new method for the green synthesis of a new nanocatalyst (Pd-NPs@FT) using Fenugreek tea in 2017.<sup>64</sup>

In this method and by stirring a solution of  $\text{PdCl}_2$  (0.01 M) with an aqueous extract of fenugreek tea (fenugreek tea due to the presence of phyto-chemical moieties, not only helps in the effective reduction of  $\text{Pd}^{(II)}$  to Pd-NPs but also helps in capping to create an excellent stabilizer against aggregation) Pd-NPs were prepared at room temperature. The reaction mixture progressively turned black, signifying the generation of Pd-NPs@FT. UV-Vis, FT-IR, and XRD confirmed  $\text{Pd}^{2+}$  reduction to crystalline  $\text{Pd}^0$  NPs by fenugreek tea extract, evidencing phenolics, proteins, polysaccharides, and other bioactive

compounds. FESEM and TEM showed 20–50 nm spherical Pd NPs uniformly coated by bio-polymer layers, preventing aggregation. SAED indicated fcc crystal structure with controlled growth along (111), demonstrating the extract's role in stabilizing and directing nanoparticles morphology.

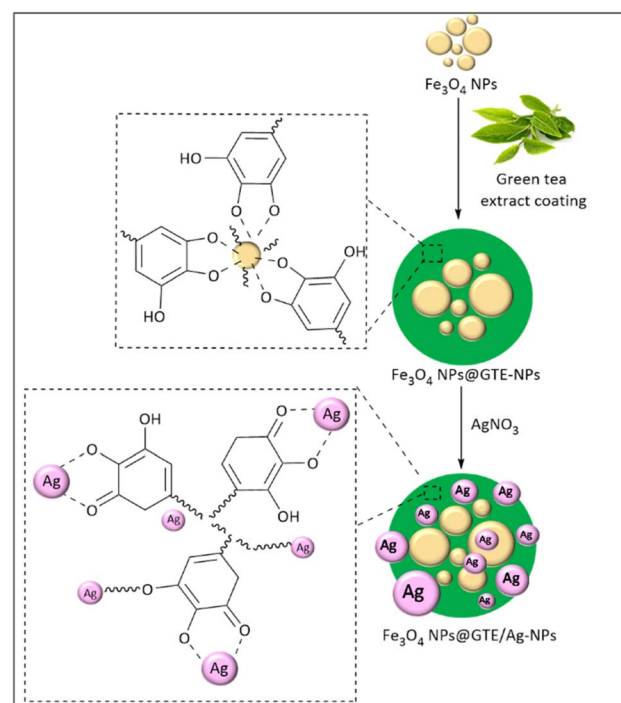
This catalyst showed high catalytic activity in the reduction of 4-nitrophenol to 4-aminophenol (Scheme 12). In this reaction, 5 mL of aqueous solution of  $\text{NaBH}_4$  (10 mM), 50  $\mu\text{L}$  of 4-nitrophenol (10 mM), and 20  $\mu\text{L}$  of the Pd-NPs@FT catalyst (1 mg  $\text{mL}^{-1}$ ) were mixed in a quartz cuvette to produce the requested product within 1 min.

In 2017, Veisi and co-worker synthesized a nanocatalyst formulated as  $\text{Fe}_3\text{O}_4@\text{GTE/Ag-NPs}$  using a green tea extract.<sup>65</sup>

To prepare the  $\text{Fe}_3\text{O}_4@\text{GTE/Ag}$  nanoparticles, deionized water was first added to green tea leaves and boiled in a water bath to obtain green tea extract. Then the mixture was cooled and filtered. In the next step, magnetite nanoparticles were dispersed in water and subjected to ultrasound. Then, green tea extract was added to the mixture to obtain a precipitate of  $\text{Fe}_3\text{O}_4@\text{GTE-NPs}$ , and after drying in a vacuum oven, they were dispersed in deionized water using an ultrasonic bath. Then  $\text{AgNO}_3$  solution was added and stirred at room temperature to ensure a complete reduction of  $\text{Ag}^{(I)}$  ions. Finally, the desired nanocatalyst ( $\text{Fe}_3\text{O}_4@\text{GTE/Ag-NPs}$ ) was prepared (Scheme 13).

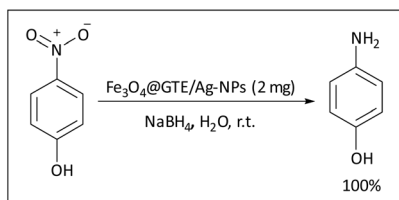
FT-IR, SEM, TEM, EDX, elemental mapping, and EDS confirmed that green tea extract (GTE) reduced  $\text{Ag}^{+}$  to  $\text{Ag}^0$  and stabilized small, spherical Ag NPs uniformly dispersed on  $\text{Fe}_3\text{O}_4$ . VSM showed a slight decrease in magnetization due to GTE and Ag coating.

The  $\text{Fe}_3\text{O}_4@\text{GTE/Ag-NPs}$  catalyst enables the reduction of 4-nitrophenol at room temperature and in water with 100%

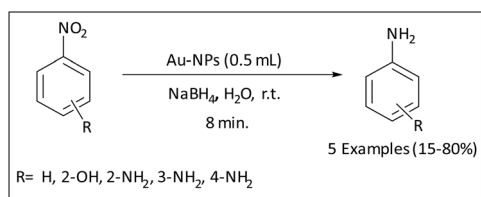


**Scheme 13** Preparation process of the  $\text{Fe}_3\text{O}_4@\text{GTE/Ag-NPs}$  catalyst.





Scheme 14  $\text{Fe}_3\text{O}_4@\text{GTE}/\text{Ag-NPs}$  as the catalyst in the reduction reaction of 4-nitrophenol to 4-aminophenol.



Scheme 15 Au-NPs catalyzed reduction of nitro aromatics by  $\text{NaBH}_4$ .

conversion by adsorbing 4-NP and  $\text{NaBH}_4$  on its surface and facilitating electron transfer. The coating of Ag nanoparticles and active functional groups such as  $\text{C}=\text{C}$  and  $-\text{OH}$  make a major contribution in the catalytic activity and create a synergistic effect (Scheme 14).

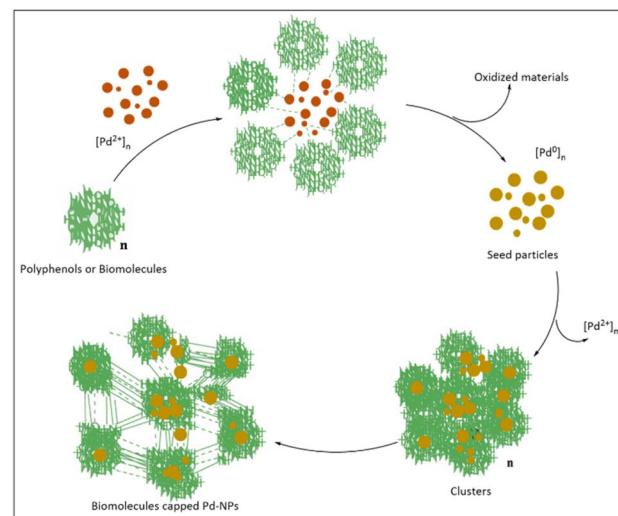
Also, the reused catalyst maintained its catalytic activity even after nine reaction cycles.

In 2018, an efficient heterogeneous catalyst (Au-NPs) was prepared during a one-step process by Alegria and co-worker.<sup>66</sup>

For this purpose, the tea solution was prepared by mixing the weight amounts of dry black tea leaves with distilled water and then vigorously stirring at room temperature. After filtration, an aqueous solution of tetrachloroauric acid ( $\text{HAuCl}_4 \cdot 3\text{H}_2\text{O}$ ) (0.1 M) was introduced into the filtrate under continuous stirring at room temperature. The solution underwent an immediate color transition from pale yellow to red, confirming the successful synthesis of gold nanoparticles.

UV-Vis and color change confirmed rapid reduction of  $\text{Au}^{3+}$  to  $\text{Au}^0$  by black tea extract. TEM/SEM showed spherical, well-dispersed Au NPs whose size increased with extract concentration, while XPS, EDS, and FTIR verified surface capping and stabilization by polyphenols and flavonoids.

In continue, the catalytic activity of the gold nanoparticles (Au-NPs) in the reduction of aromatic nitro compounds was investigated in aqueous solution. The results showed that Au-NPs are efficient in the studied reduction reaction (Scheme 15), and the catalytic activity depends on the concentration of the catalyst and sodium borohydride, while the reaction kinetics follows a pseudo-first order law. Also, using this method, the reduction of other nitro compounds, including nitroanilines and nitrobenzene, was studied. In general, compounds bearing the nitro group at the 4-position showed higher conversion rates (77%), followed by 2-position nitro compounds (40%) and 3-position nitro compounds (15%).



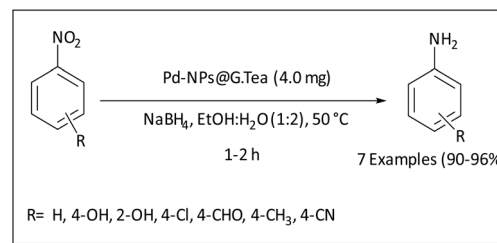
Scheme 16 Proposed reaction pathway for the synthesis of Pd-NPs.

Recycling studies for Au-NPs as a catalyst in the reduction of 4-NP showed that the catalyst can be recycled up to 4 times.

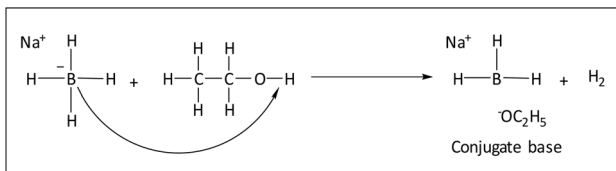
Veisi and co-workers synthesized a Pd-NPs@G.Tea extract heterogeneous catalyst by a facile and green route.<sup>67</sup> In this study and in order to obtain tea extract, fresh green tea leaves which were collected from northern Iran were washed three times with double distilled water before use. Then, after adding deionized water, it was boiled in a water bath and filtered through filter paper Whatman No. 1. Polyols and carbonyl groups in green tea aqueous extract act as reducing and capping/stabilizing agents. To prepare Pd-NPs, the prepared plant extract was added dropwise to 1 mM  $\text{PdCl}_2$  aqueous solution and the mixture was refluxed. The color of the reaction mixture was gradually changed, indicating the formation of Pd nanoparticles, and the catalyst was precipitated after adding acetone to reach to Pd-NPs@G.Tea (Scheme 16).

UV-Vis showed  $\text{Pd}^{2+}$  reduction to  $\text{Pd}^0$  by green tea extract. TEM and FESEM confirmed the presence of small (7–10 nm), spherical, and well-dispersed Pd NPs coated with a bio-polymer layer from the extract, preventing aggregation. FT-IR, EDS, and XRD verified surface capping, stabilization by polyphenols, flavonoids, and polysaccharides, and crystalline  $\text{Pd}^0$  formation.

In continue, the catalytic performance of this reagent in nitroarene reduction was investigated. Firstly, the reduction of nitrobenzene using  $\text{NaBH}_4$  served as a model reaction to assess the catalytic efficiency of Pd-NPs@G.Tea. The best result was



Scheme 17 Nitroarenes reduction catalyzed by Pd-NPs@G.Tea.



Scheme 18 Reduction of nitrobenzene *via* the reaction between ethanol and  $\text{NaBH}_4$  and the production of  $\text{H}_2$  gas.

obtained using 4.0 mg of the catalyst, for the reduction of 1.0 mmol nitrobenzene in the presence of 2.0 mmol  $\text{NaBH}_4$  in a mixture of ethanol and water (1 : 2) at 50 °C. Then, the catalytic application for nitroarenes containing electron-donating and electron-withdrawing groups was investigated and the enhanced catalytic activity was inferred due to the high surface area and hydrogen trapping ability of the catalyst. These features can help in the treatment of wastewater contaminated with *p*-nitrophenol in industries (Scheme 17).

In this study, the reusability of the catalyst was also tested in the reduction of nitrobenzene with  $\text{NaBH}_4$ , showing its stability at least for six consecutive reaction cycles without significant loss of activity.

This reaction can be done by the conversion of ethanol to ethoxide ion in reaction with  $\text{Na}^+ \text{BH}_4^-$  to form hydride ester and hydrogen gas (Scheme 18).

## Two-component catalytic reactions

**A: Suzuki–Miyaura reaction.** Biaryl moieties are key building blocks in numerous important compounds, including drugs, agrochemicals, natural products, and advanced materials such as conductive polymers, molecular wires, and liquid crystalline compounds.<sup>68</sup> Their synthesis typically involves the formation of carbon–carbon bonds, which can be efficiently achieved through various coupling reactions, which of them Kumada, Heck, Negishi, Suzuki–Miyaura, Stille–Migita–Kosugi, Sonogashira, and Hiyama are examples.<sup>69,70</sup>

Among these, the Suzuki–Miyaura reaction has gained widespread popularity in both laboratory and industrial settings.<sup>71</sup> In 1979, Akira Suzuki discovered this reaction, and because of this, he was awarded the Nobel Prize in Chemistry in 2010. Norio Miyaura, in collaboration with Akira Suzuki, helped to the development of the Suzuki reaction, which after that named as the Suzuki–Miyaura cross-coupling reaction.<sup>72,73</sup> The Suzuki–Miyaura cross-coupling involves the reaction of

a boronic acid with an aryl or vinyl halide in the presence of a palladium catalyst, proceeding through three main steps: oxidative addition, transmetalation, and reductive elimination.<sup>74,75</sup>

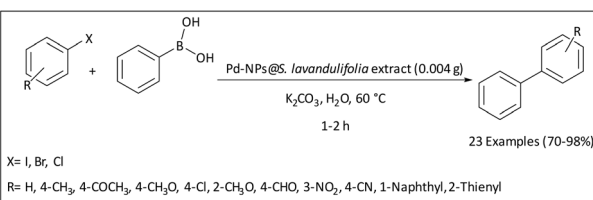
Palladium facilitates the reaction by activating both the boron-containing molecules and the organic halides (vinyl or aryl halide), bringing them into close proximity and ensuring high selectivity, which enhances product purity and minimizes side reactions.<sup>76–78</sup>

The reason behind the spread of the Suzuki reaction is the use of borons and aryl boronic acids, which are stable, quite affordable, and compatible with almost all functional groups and by using these materials, it is possible to do the reaction in all kinds of solvents under mild conditions.<sup>79</sup> In addition, because organoboranes are compounds resistant to air humidity with low toxicity, the Suzuki coupling reaction is a method to replace other methods that use organometallics.<sup>71</sup> For this reason, the Suzuki–Miyaura reaction has become the second most used reaction in drug discovery and development. For example, this reaction can be used to prepare caparratriene as a natural product that is robustly active against leukemia, from derivatives of cirronellal. On the other hand, this reaction can be performed to prepare fine chemicals *via* aryl halides.<sup>80,81</sup> In the field of materials science, the reaction enables the construction of advanced functional materials such as light-emitting polymers, polymers for insulating electronic chips, and compounds for organic light-emitting diodes.<sup>82–84</sup> Despite these broad applications and advantages, including wide substrate scope, high functional group tolerance, and excellent yields, several challenges still remain. The high cost and limited availability of palladium, the challenges in activating aryl chlorides, and the environmental impact of organic solvents have prompted the search for greener alternatives. These include ligand-free protocols, the use of earth-abundant transition metals, and biogenic nanocatalysts derived from natural products such as tea extracts, which offer improved sustainability. In this context, bioactive compounds such as flavonoids and polyphenols present in the extracts not only serve as reducing agents but also act as stabilizers and capping agents, providing surface coverage that enhances the stability and uniformity of the nanoparticles.<sup>72,85</sup>

For the first time in 2015, Veisi and co-workers reported a successful green approach for the synthesis of  $\text{Pd-NPs}@\text{S. lavandulifolia}$  catalyst using the aqueous extract of herbal tea (*Stachys lavandulifolia*) to promote the Suzuki–Miyaura reaction.<sup>80</sup>

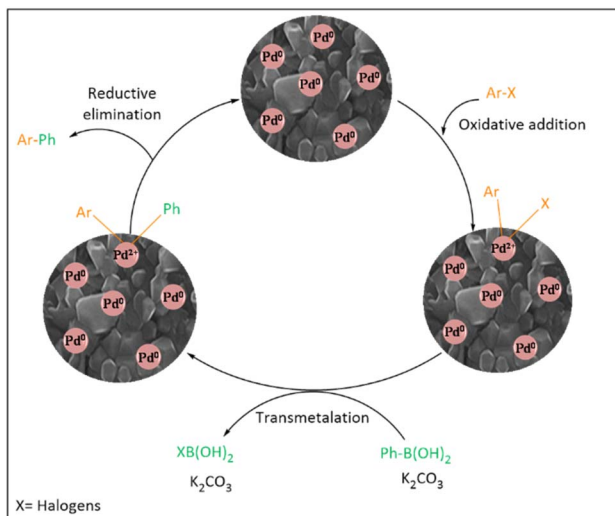
To prepare the catalyst, freshly collected herbal tea from Kermanshah, Zagros region (Iran), after washing and drying, was added to Milli-Q water, then the extract was filtered through Whatman No. 1 filter paper and centrifuged for 5 minutes to remove unwanted aggregates. In continue a solution of  $\text{PdCl}_2$  (1 mM) was added to the extract and refluxed. The emersion of a dark color indicates the formation of Pd-NPs. After adding acetone (anti-solvent), the catalyst ( $\text{Pd-NPs}@\text{S. lavandulifolia}$  extract) was precipitated.

In this study, UV-vis showed  $\text{Pd}^{2+}$  reduction by the tea extract, FTIR evidenced tea phytochemicals in capping, TEM/



Scheme 19 Suzuki–Miyaura cross-coupling reaction using  $\text{Pd-NPs}@\text{S. lavandulifolia}$  extract.





Scheme 20 Possible mechanism of the Suzuki–Miyaura coupling reaction.

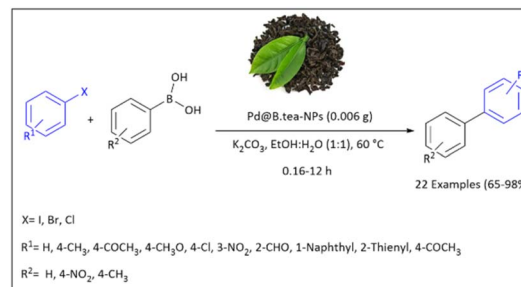
SEM revealed uniform spherical PdNPs, and XRD confirmed crystalline  $\text{Pd}^0$  while EDX evidenced Pd with C and O from tea organics attached to the nanoparticle surface. Then, the Suzuki–Miyaura coupling reaction between bromobenzene and phenylboronic acid under optimized conditions ( $\text{K}_2\text{CO}_3$ , water solvent, 60 °C and 0.004 g of the catalyst) was studied (Scheme 19). This catalytic system was applicable to various aryl halides (iodides, bromides, and chlorides). The coupling reactions of aryl iodides and bromides with phenylboronic acid generally proceeded in excellent yields of 95–98% within 1–7 h. In contrast, the reactions of aryl chlorides required longer reaction times (15–18 h) and afforded only moderate yields of 70–75%, which can be attributed to the stronger C–Cl bond. Furthermore, the Suzuki–Miyaura cross-coupling of heteroaryl halides such as 2-iodothiophene (1.2 h, 98%) and 2-bromothiophene (5 h, 92%), as well as sterically congested *ortho*-halides like 2-iodoanisole (3 h, 98%) and 2-bromoanisole (7 h, 90%), and the bulky 1-iodonaphthalene (4 h, 96%), also proceeded efficiently to give the corresponding products in good to excellent yields under the optimized conditions.

In this study, the catalyst was easily separated from the products and reused up to eight times without the considerable loss of its activity.

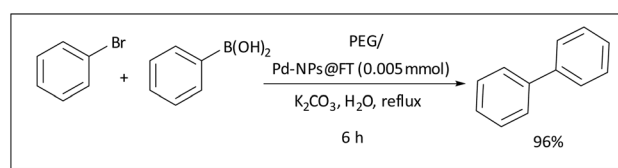
The reaction mechanism for the Suzuki–Miyaura coupling reaction using (Pd-NPs@*S. lavandulifolia* extract) as the nanocatalyst is presented in Scheme 20.

In the other discussion on the reduction of nitrophenols, the preparation of the Pd@B.tea-NPs catalyst using a green route with natural black tea leaf extract (*Camellia sinensis*) was described in 2017 by Lebaschi *et al.*<sup>63</sup>

After characterization, the Pd@B.tea-NPs catalyst was used as an efficient and heterogeneous catalyst in the Suzuki–Miyaura coupling reaction between phenylboronic acid and a range of aryl halides ( $X = \text{I, Br, Cl}$ ), in which the reaction with



Scheme 21 Suzuki–Miyaura coupling reaction in the presence of Pd@B.tea-NPs.



Scheme 22 Suzuki–Miyaura coupling reaction catalyzed by Pd-NPs@FT.

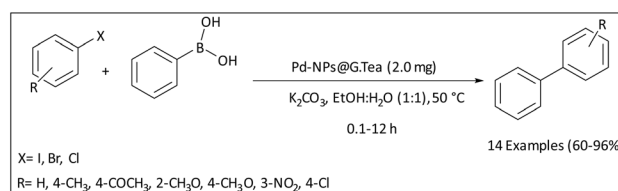
aryl chlorides required a longer reaction time (12 h) to produce the desired products in moderate yields (65–75%) (Scheme 21).

The obtained results showed that under the selected conditions the dried recycled catalyst could be used consecutively for five cycles without significant loss of activity. The mechanism of these reactions is based on that shown in Scheme 20, although the catalyst differs.

As explained in the previous section, Mallikarjuna and co-workers in 2017 reported the synthesis of Pd-NPs@FT as a green catalyst through an environmentally friendly method. This catalyst, not only was used in the reduction of nitrophenols as explained before, but also acts as an effective and highly stable catalyst in the Suzuki–Miyaura reaction.<sup>64</sup> In this work, the requested coupling reaction resulted in the desired biphenyl in 96% yield within 6 h (Scheme 22).

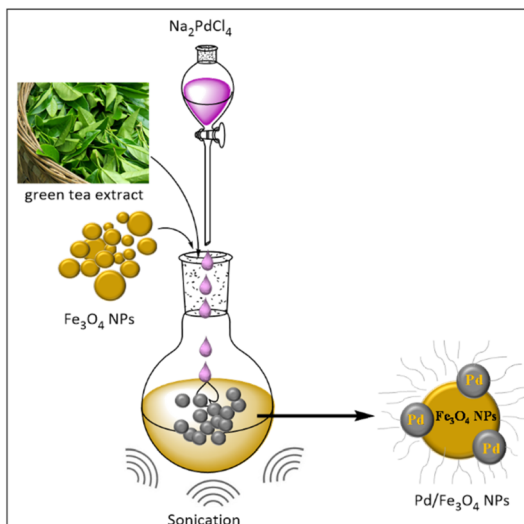
In the previous section, we have seen that the Pd-NPs@G.Tea catalyst can play an efficient role in the reduction of nitro compounds (Scheme 17). Further studies clarified that this reagent can also be used for the promotion of the Suzuki–Miyaura reaction (Scheme 23).<sup>65</sup>

In this investigation and under the optimal reaction conditions (2.0 mg catalyst, 2.0 mmol  $\text{K}_2\text{CO}_3$ , ethanol–water (1 : 1), 50 °C, 0.1–12 h), the Suzuki–Miyaura coupling reaction was performed using Pd-NPs@G.Tea as a catalyst.



Scheme 23 Suzuki–Miyaura cross-coupling reaction in the presence of Pd-NPs@G.Tea.





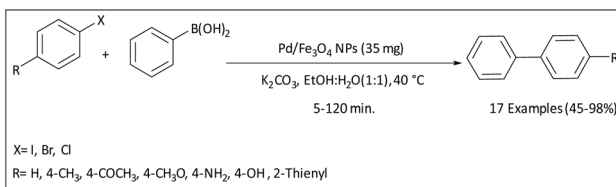
**Scheme 24** Preparation of Pd/Fe<sub>3</sub>O<sub>4</sub> NPs assisted by green tea extract under ultrasonic irradiations.

°C), a wide range of aryl halides (I, Br, Cl) were reacted with phenylboronic acid. In this context, the coupling reactions of aryl iodides and bromides were completed within 0.1–4 h, whereas reactions with aryl chlorides required a longer time of 12 h, because that the breaking of the C–Cl bond requires more energy leading to its less reactivity.

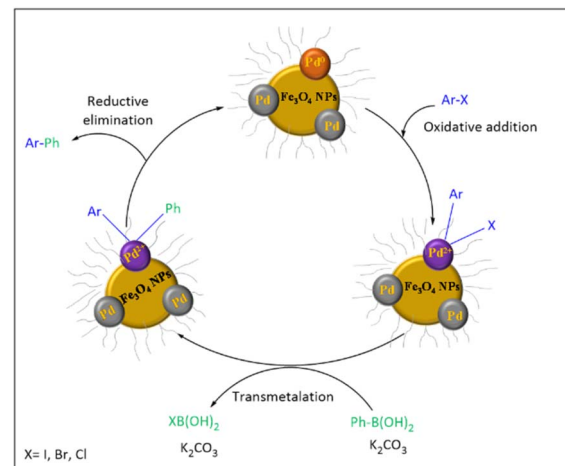
The studies related to the reusability of the introduced heterogeneous catalyst in the reaction of bromobenzene and phenylboronic acid showed that the catalyst can be recycled 7 times without significant loss of its activity.

In 2019, Pd/Fe<sub>3</sub>O<sub>4</sub> NPs was prepared as a nanocatalyst by Veisi and co-workers *via* a new and efficient approach using green tea extract.<sup>86</sup> At first, after taking samples of green tea leaves from the north of Iran, the research group prepared an aqueous extract from the leaves. In the next step, the magnetite nanoparticles were subjected to ultrasound after being dispersed in water. Then, the green tea extract was added to the mixture, and under sonication, a solution of Na<sub>2</sub>PdCl<sub>4</sub> in water was added dropwise to it using a drop funnel. Then, a magnet was used for the magnetic separation of the nanoparticles of Pd/Fe<sub>3</sub>O<sub>4</sub> NPs from the solution as a dark solid (Scheme 24).

FT-IR confirmed that phenolic and flavonoid groups are responsible for Pd<sup>2+</sup> reduction and stabilization. TEM/FESEM showed well-dispersed Pd NPs coated by tea biomolecules while XPS/XRD verified Pd<sup>0</sup> formation and crystalline structure.



**Scheme 25** The Suzuki–Miyaura reaction using Pd/Fe<sub>3</sub>O<sub>4</sub> NPs as the catalyst.



**Scheme 26** Possible mechanism of the Suzuki–Miyaura coupling reaction using Pd/Fe<sub>3</sub>O<sub>4</sub> NPs as the catalyst.

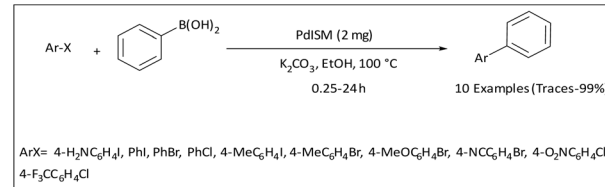
Also EDX detected C/O from tea on the surface, and VSM/BET indicated retained magnetic properties and a suitable active surface.

In continue, the catalytic activity of Pd/Fe<sub>3</sub>O<sub>4</sub> NPs as a new magnetic and heterogeneous catalyst in the Suzuki–Miyaura coupling reactions under the influence of ultrasound was evaluated (Scheme 25). It was found that this method is very effective in converting aryl halides (I, Br and Cl) to the desired biphenyl compounds with significant efficiency (45–98%) during short reaction times (5–120 min). In addition, the recovery of the Pd/Fe<sub>3</sub>O<sub>4</sub> NPs catalyst was evaluated, which showed that this catalyst remains reusable through a minimum of six consecutive cycles.

The probable mechanism of the Suzuki–Miyaura coupling reaction in the presence of the Pd/Fe<sub>3</sub>O<sub>4</sub> NPs nanocatalyst is shown in Scheme 26.

In a 2021 report, Schmitt and co-workers introduced a PdISM catalyst containing palladium nanoparticles *via* biological reduction using *Ilex paraguariensis* aqueous extract.<sup>87</sup>

To prepare the catalyst, at first, the sample of *Ilex paraguariensis* (a very widespread tea in southern South America) was added to deionized water. The mixture was placed in a thermostatic bath and filtered to prepare yerba mate aqueous extract. The aqueous solution of PdCl<sub>2</sub> was dripped into the aqueous extract of *Ilex paraguariensis* in an ultrasonic bath at low speed. Finally, the solution was washed with acetone to remove the green color and centrifuged to obtain a black precipitate (PdISM).



**Scheme 27** The Suzuki–Miyaura cross-coupling reaction catalysed by PdISM.

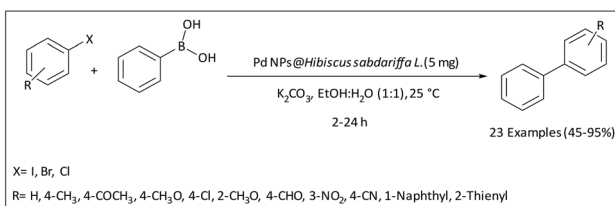
FT-IR and color change confirmed that phenolic and carbonyl groups in *Yerba Mate* extract reduced  $\text{Pd}^{2+}$  to  $\text{Pd}^0$  and stabilized the nanoparticles, TEM showed well-dispersed Pd NPs without agglomeration, XRD verified fcc crystalline Pd, and ICP-OES indicated incorporation of natural mineral elements from the extract. After the identification, PdISM was employed as an efficient catalyst to achieve outstanding yields in the coupling reactions of aryl iodides, bromides, and chlorides with phenylboronic acid (Scheme 27). The results showed that under these conditions, aryl iodides reacted within 0.25–1 h, whereas aryl bromides and chlorides required longer reaction times of 20–24 h to be converted to the desired products.

The reusability of PdISM was further examined in the coupling of 4-iodoaniline and phenylboronic acid under optimized conditions, demonstrating that the catalyst could be recovered and reused at least three times without significant loss of its activity.

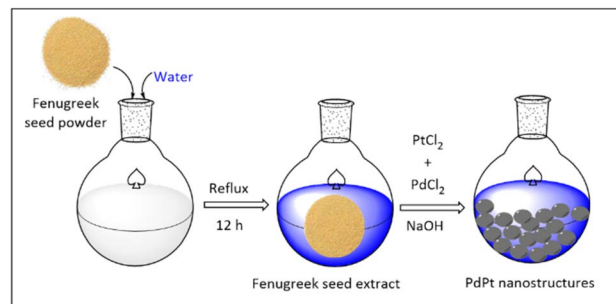
In 2017, Hekmati *et al.* designed a simple and environmentally friendly method for the biosynthesis of the Pd NPs@*Hibiscus sabdariffa* L. catalyst using red tea (*Hibiscus sabdariffa* L.) aqueous extract as a reducing and stabilizing agent.<sup>88</sup> In this study, freshly collected red tea (*Hibiscus sabdariffa* L.) was washed, dried and used to prepare the extract. The extract was added to Milli-Q water and after heating, it was filtered through Whatman No. 1 filter paper and then subjected to centrifugation for aggregate removal. A solution of  $\text{PdCl}_2$  was added to the prepared extract. The appearance of dark color indicated the formation of the Pd nanoparticles.

UV-Vis/color change and FT-IR confirmed that phenolic and flavonoid compounds in hibiscus extract reduced  $\text{Pd}^{2+}$  to  $\text{Pd}^0$  and stabilized the nanoparticles, TEM/SEM showed well-dispersed spherical Pd NPs (5–8 nm) coated with biomolecules, XRD verified crystalline  $\text{Pd}^0$ , and EDX/EDX mapping confirmed Pd formation, its uniform distribution, and surface carbon from hibiscus, confirming effective dispersion by the extract.

In continue, the catalytic activity of Pd NPs@*Hibiscus sabdariffa* L. was evaluated for the Suzuki–Miyaura cross-coupling reaction in a water–ethanol solvent system (Scheme 28). After optimizing the reaction conditions (0.2 mol% of the catalyst, 2 mmol of  $\text{K}_2\text{CO}_3$ , 2 mL of  $\text{H}_2\text{O}$ –EtOH (1:1), 25 °C), a wide range of aryl halides (I, Br, Cl) and phenylboronic acid were coupled in good to excellent yields (45–95%) and variable reaction times (2–24 h) using this method. The research group was also studied the reusability of Pd NPs@*Hibiscus sabdariffa* L. in the reaction of bromobenzene and



Scheme 28 Suzuki–Miyaura coupling reaction catalysed by Pd NPs@*Hibiscus sabdariffa* L. as catalyst.



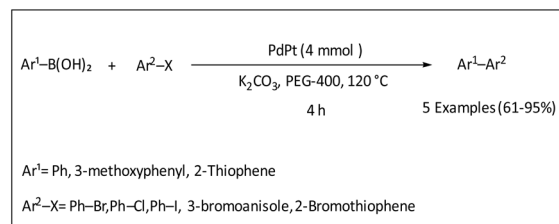
Scheme 29 Using fenugreek seed extract to prepare the PdPt nanocatalyst.

phenylboronic acid. The results showed unchanged catalytic behavior for up to five reactions.

In other study bimetallic palladium–platinum (PdPt) nanoparticles were synthesized through polysaccharides derived from fenugreek with a simple method by Bathula and co-workers in 2024.<sup>89</sup>

To prepare the PdPt nano catalyst, fenugreek seed powder was soaked in deionized water and heated. The extract was centrifuged and then stored in a refrigerator to settle the undissolved material and drain the clear upper solution. Then it was filtered through filter paper. An aqueous solution containing 1 mM platinum chloride was added to the prepared extract solution. To form nanoparticles, the reaction mixture was stirred for 24 hours at 90 °C. The color of the reaction mixture turns into a dark solution, which indicates the formation of the PdPt nanocatalyst (Scheme 29). Further studies using XRD confirmed the crystalline PdPt phase and phase purity, while TEM/SEM showed nanometer-sized PdPt particles shielded by polysaccharide biopolymers. XPS verified PdPt formation and surface coverage with C, N, and O from polysaccharides.

Then, the PdPt catalyst was used as a promotor in the Suzuki–Miyaura coupling reaction between organic halides and boronic acids (Scheme 30). Under the optimized conditions (120 °C, PEG-400 as a solvent, 4 mol% catalyst), the reaction of phenylboronic acid and bromobenzene as a model was completed within 4 h. The effect of different halogen substituents was also examined, and while chlorobenzene afforded a relatively lower yield (61%), iodobenzene gave the corresponding biaryl product in 95% yield, consistent with the higher reactivity of the C–I bond compared to the stronger C–Cl bond. Under the selected conditions the products, such as 3,3'-



Scheme 30 Suzuki–Miyaura coupling reaction investigated in the presence of PdPt.



dimehoxy biphenyl (93%) and bithiophene (94%) were also prepared in high yields. In addition, the nanocatalyst was recycled up to 5 times, showing its considerable stability during the course of the reaction.

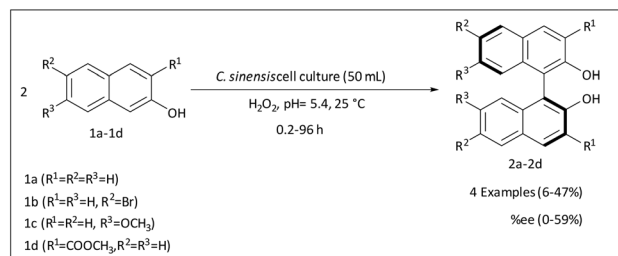
**B: other two-component reactions.** In general, tea-derived nanocatalysts have proven to be versatile and efficient for a wide range of two-component reactions, including heterocycle synthesis, C–O/C–N/C–heteroatom couplings, *O*-acetylation, and biaryl formation. These catalysts leverage the inherent polyphenols and flavonoids in tea, whose hydroxyl and carbonyl groups act as reducing and stabilizing agents for the formation and surface functionalization of metal nanoparticles. Operating under mild and eco-friendly conditions, they exhibit high selectivity, excellent yields, broad substrate tolerance, and notable recyclability. Despite challenges such as substrate electronic effects and optimization requirements, tea-mediated systems offer a sustainable alternative to conventional catalysts, combining green chemistry principles with robust performance, operational simplicity, and applicability to both pharmaceutical and organic synthesis contexts.

1,1-Binaphthalene derivatives are widely used in organic synthesis as chirality inducers for selective reactions.<sup>90–92</sup> One method for the preparation of pure binaphthyl derivatives is catalytic oxidative coupling.<sup>93</sup> In this area, enantioselective oxidation of 2-naphthols leads to 1,1-binaphthyl-2,2-diols.<sup>94</sup>

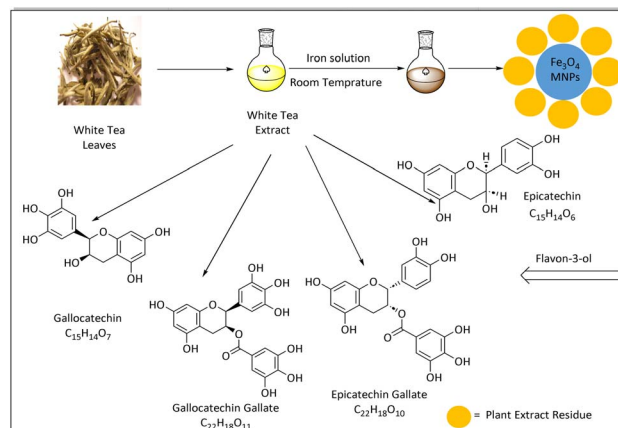
In 2002, Takemoto and co-workers reported the production of photoactive 1,1-binaphthyl-2,2-diols by enantioselective oxidative coupling of 2-naphthol derivatives using *Camellia sinensis* cell culture.<sup>95</sup>

To prepare the *Camellia sinensis* cell culture catalyst, first, *C. sinensis* cells (4.6 g of cells, 20 mL of broth) were cultured in B5 medium (a nutrient blend of inorganic salts, vitamins and carbohydrate) (60 mL) for 12 days as the stationary phase to prepare free cells from *Camellia sinensis*. In the next step, to make the ICSC (immobilized *Camellia sinensis* cell culture) catalyst, 5% sodium alginate solution (80 mL) was mixed with free cells. The resulting mixture was added dropwise to a 0.6% calcium chloride solution (1000 mL). After washing with water, the immobilized cell catalyst (ICSC) was obtained. Then, for the ICSC culture and incubation, ICSC cells (7 g cells and 30 mL medium) were added to fresh B5 medium (80 mL per flask). The cell culture was performed at 25 °C with a shaker (110 rpm) in the dark. Next, various 2-naphthol derivatives underwent oxidative coupling reaction using *Camellia sinensis* cell culture (Scheme 31). According to the results, it was shown that the presence of Br, OMe or COOMe groups on the naphthalene ring decreases the enantioselectivity and chemical performance. While unsubstituted 2-naphthol gave 47% and 59% ee with the *R* enantiomer, the substituted derivatives afforded lower yields (6–34%) and reduced ee values (0–36%) with the *S* enantiomer.

Heterocyclic compounds are among the largest and most diverse organic compounds.<sup>96</sup> Among the heterocycles, benzimidazoles are an important group of nitrogen-containing heterocycles.<sup>97</sup> These compounds are very important intermediates in the construction of biologically and medicinally active molecules, so they are very important in organic chemistry.<sup>98,99</sup>



Scheme 31 Enantioselective oxidative dimerization of 2-naphthols employing *C. sinensis* cell culture.



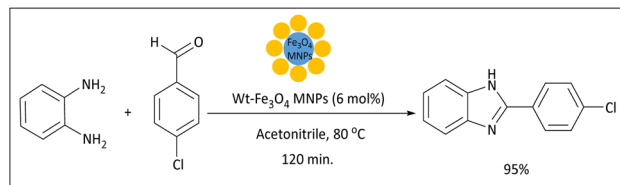
Scheme 32 Synthesis of Wt- $Fe_3O_4$  MNPs using white tea extract.

In 2017, Shojaee and co-workers reported for the first time the synthesis of 2-(4-chlorophenyl)-1*H*-benzo[*d*]imidazole using the synthesized Wt- $Fe_3O_4$  MNPs as a stable and heterogeneous nanocatalyst.<sup>100</sup>

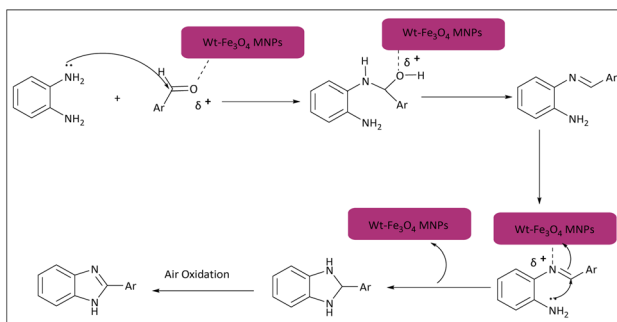
To prepare Wt- $Fe_3O_4$  MNPs as a nanocatalyst, white tea was washed and dried to remove possible impurities. After that, it was ground into the powder, boiled, and stirred with deionized distilled water in an Erlenmeyer flask and then filtered by a vacuum pump. In the next step, 2 moles of  $FeCl_3 \cdot 6H_2O$  and 1 mole of  $FeCl_2 \cdot 4H_2O$  were dissolved in ionized water with a molar ratio of 2 : 1 under a nitrogen atmosphere and then the aqueous extract of white tea was added to it. After the complete biological reduction of the ions, the mixture was centrifuged to separate the black powder of Wt- $Fe_3O_4$  MNPs from the compounds in the solution (Scheme 32). In this research, FT-IR confirmed the involvement of phenolic and flavonoid groups from white tea in  $Fe^{3+}$  reduction and nanoparticle stabilization. XRD showed both crystalline  $Fe_3O_4$  and a broad peak from natural compounds of the extract. EDX verified Fe signals along with C and O, indicating the extract coating on the nanoparticle surface.

In continue, through one-pot condensation of *o*-phenylenediamines with 4-chlorobenzaldehyde, the effectiveness of the synthesized catalyst was investigated (Scheme 33). The obtained results clarified that with 6 mol% of the catalyst at 80 °C, in acetonitrile, and during 120 minutes, the reaction can be proceeded with 96% yield.





**Scheme 33** Synthesis of 2-(4-chlorophenyl)-1*H*-benzo[*d*]imidazole catalyzed by Wt- $\text{Fe}_3\text{O}_4$  MNPs.



**Scheme 34** Proposed mechanism for the synthesis of 2-substituted benzimidazoles using Wt- $\text{Fe}_3\text{O}_4$  MNPs.

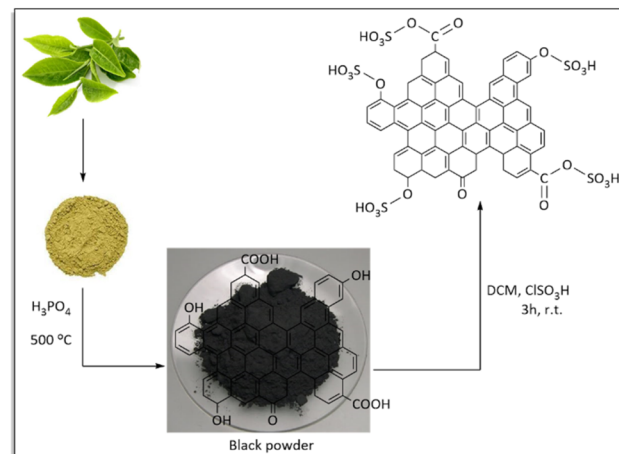
Under the selected conditions the Wt- $\text{Fe}_3\text{O}_4$  MNPs catalyst can be recovered using an external magnetic field and could be used up to 5 times without significant loss of its catalytic activity.

The probable mechanism for the formation of 2-substituted benzimidazole compounds from the condensation reaction between *o*-phenylenediamine and benzaldehyde derivatives in the presence of the heterogeneous Wt- $\text{Fe}_3\text{O}_4$  MNPs catalyst is shown in Scheme 34.

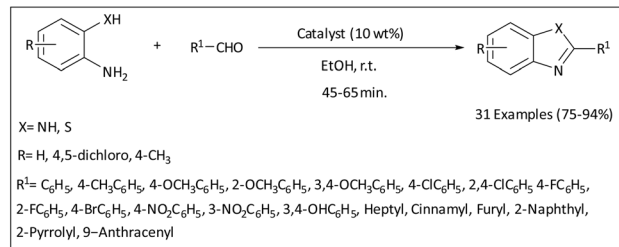
Benzimidazoles and benzothiazoles are used as the backbone of many important biologically active molecules, including anti-parasitic, anti-fungal, anti-viral and anti-tumor drugs.<sup>101</sup> Due to the widespread use of these heterocycles, their synthesis have been widely studied.<sup>102</sup>

In this line, an efficient and simple eco-friendly approach for the synthesis of 2-substituted benzimidazoles and benzothiazoles using sulfonic-acid-functionalized carbon, (which was prepared from mature tea leaves (MTLAC-SA)) was reported by Goswami and co-workers in 2018.<sup>103</sup>

To prepare this heterogeneous catalyst, mature tea leaves (MTL) were first thoroughly washed with distilled water to remove impurities, then dried, ground and sieved to prepare the activated carbon. MTL powder was soaked in 85%  $\text{H}_3\text{PO}_4$  and carbonized in a tube furnace under nitrogen atmosphere. After cooling to room temperature, activated carbon was washed, dried, ground, and sieved to reach the MTLAC. In the next step, MTLAC powder was dispersed in dry  $\text{CH}_2\text{Cl}_2$  by ultrasonic bath and by adding chlorosulfonic acid dropwise to this solution at room temperature and stirring the mixture for 3 hours, sulfonic acid activated carbon (MTLAC-SA) was obtained (Scheme 35). BET and SEM analyses confirmed the porous morphology and



**Scheme 35** Schematic of MTLAC-SA synthesis.



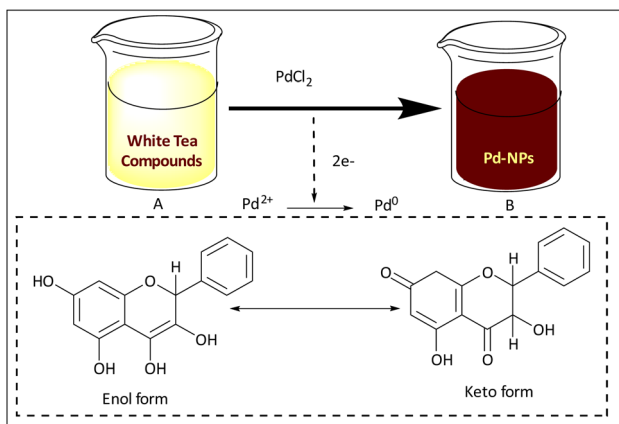
**Scheme 36** Use of MTLAC-SA as the catalyst to synthesize benzimidazole and benzothiazole derivatives.

high surface area of the tea-derived activated carbon. EDX revealed C and O from the tea source, along with additional S signals (indicative of  $-\text{SO}_3\text{H}$  groups), confirming successful sulfonic acid functionalization. FT-IR further detected characteristic bands of sulfonic acid groups, while Boehm titration verified the increased surface acidity.

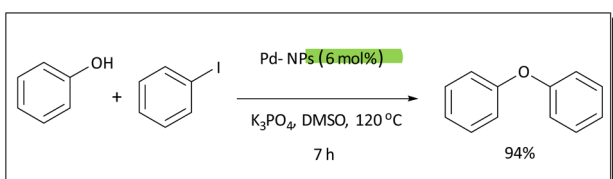
The reaction of 4-methylbenzaldehyde with *o*-phenylenediamine in the presence of MTLAC-SA catalyst was chosen as a model reaction to confirm its catalytic ability and the influence of various solvent systems for the synthesis of the imidazole derivatives was investigated on it. The results obtained in EtOH and acetonitrile were almost equal; considering the environmental effects, ethanol was selected as the solvent. The optimal catalyst loading was also determined. Using 10 wt%, 92% of the product is produced in 45 minutes. The flexibility of this approach was examined by conducting the reaction with diverse substituted aldehydes. Under the optimized conditions, the selected aldehydes with both electron-donating and electron-withdrawing substituents were successfully converted to their corresponding derivatives in 75–94% yields (Scheme 36).

To check the recyclability of the catalyst, the reaction between 4-methylbenzaldehyde and *o*-phenylenediamine was repeated in the presence of the recycled MTLAC-SA successfully for seven catalytic cycles without considerable decrease in the product yield, and change in the reaction time.





Scheme 37 The aqueous extract of white tea (A) before and (B) after the synthesis of Pd-NPs.



Scheme 38 Diaryl ether formation reaction.

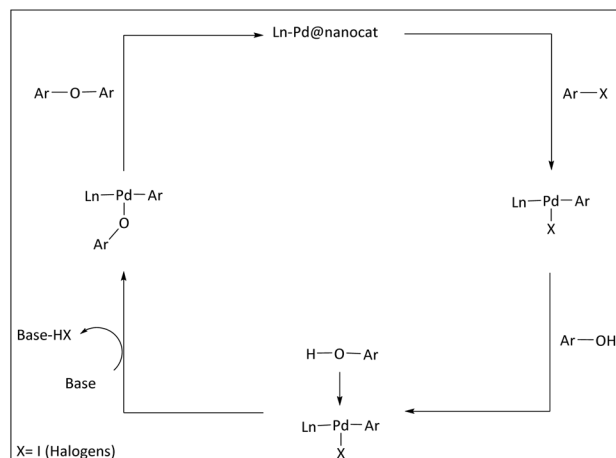
Diaryl ether (DE) is a functional scaffold which is widely observable in natural products and synthetic organic compounds. Due to its excellent properties, the DE core has been recognized as an essential element of pharmaceutical and agrochemical agents with various biological targets.<sup>104</sup>

For this reason, Mahdavi Shahri prepared a highly efficient and stable heterogeneous nanocatalyst (Pd@nanocat) for the synthesis of diaryl ether.<sup>105</sup>

In this study and as the first step, to prepare the Pd@nanocat, white tea was washed several times with distilled water to remove impurities, and then dried to remove moisture, and turned into powder. The white tea powder sample was dispersed in distilled water with magnetic stirring and then heated. The extract was cooled to room temperature and filtered through filter paper. In the next step, Erlen containing PdCl<sub>2</sub> solution (1 mM) was mixed with the aqueous extract of white tea, and the color of the reaction mixture gradually changed from yellow to dark brown indicating the formation of palladium nanoparticles. The solid product was collected by centrifugation, and after washing with distilled water, the black powder of Pd@nanocat was dried in an oven (Scheme 37).

Color change confirmed Pd<sup>2+</sup> reduction by white tea extract. XRD showed fcc Pd peaks and a broad  $2\theta \approx 13.5^\circ$  peak from tea compounds. SEM, TEM, and EDX revealed well-dispersed Pd NPs coated with extract molecules, ensuring stability and morphology control *via* hydrogen bonding and electrostatic interactions.

Then, the synthesis of diaryl ether was evaluated from the cross-coupling reaction of iodobenzene with phenol in the



Scheme 39 Plausible mechanism for the catalytic synthesis of diaryl ether.

presence of dimethyl sulfoxide (DMSO) as a solvent at 120 °C under N<sub>2</sub> atmosphere using 6 mol% of Pd@nanocat (Scheme 38).

The reusability and recyclability of the catalyst was also investigated and the recycled catalyst was used consecutively for four runs without significant loss of its performance.

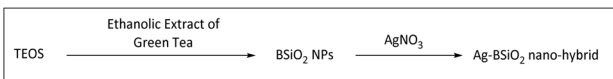
The proposed mechanism of C–O coupling reaction for diaryl ether synthesis under the effect of the Pd@nanocat catalyst is shown in Scheme 39. This mechanism involves three main steps: oxidative addition, transmetalation, and reductive elimination, leading to the formation of a C–O bond and re-production of the active Pd<sup>0</sup> L<sub>2</sub> species.

Organic compounds containing quinoline scaffolds have been widely studied due to their many applications as bioactive molecules. Dihydroquinoline derivatives include a large family of important medicinal compounds and are used in the production of antihypertensive, antidiabetic, antitumor, and many other drugs.<sup>106,107</sup> Due to their wide biological activities, multiple approaches for preparing these compounds have been documented. Nevertheless, the existing methods suffer from notable limitations, including severe reaction conditions, sluggish reaction kinetics, and the inability to recycle the catalysts.<sup>108</sup>

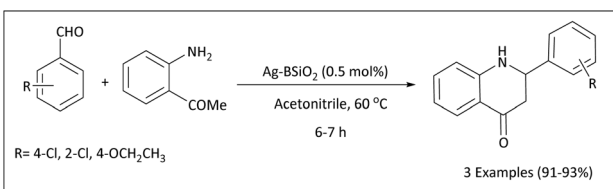
Therefore, in 2019 Otari and co-workers proposed a silver nanoparticle-decorated biomolecule-entrapped SiO<sub>2</sub> (Ag–BSiO<sub>2</sub>) nanohybrid catalyst made by the use of green tea biomolecules to overcome the limitations mentioned above.<sup>109</sup>

To prepare the Ag–BSiO<sub>2</sub> hybrid nanostructures, green tea leaf ethanol extracts were prepared by mixing 1.2 grams of tea leaves in 40 mL of pure C<sub>2</sub>H<sub>5</sub>OH. After mixing and centrifugation, the extract was purified and stored at 4 °C. For the synthesis of SiO<sub>2</sub> nanoparticles, 2 mL of tetra ethyl orthosilicate (TEOS) was added dropwise to C<sub>2</sub>H<sub>5</sub>OH, and then ammonium hydroxide was added and the solution was stirred for 24 hours. Then, the SiO<sub>2</sub> nanoparticles were washed with water and dried. For the synthesis of BSiO<sub>2</sub> nanoparticles, TEOS was added to the purified ethanol green tea extract and stirred with ammonium





**Scheme 40** The synthetic diagram for the preparation of Ag-BSiO<sub>2</sub> catalyst.



**Scheme 41** Synthesis of dihydroquinolines in the presence of Ag-BSiO<sub>2</sub>.

hydroxide for 12 hours. Finally, in order to receive to the Ag-BSiO<sub>2</sub> hybrid structures, BSiO<sub>2</sub> nanoparticles were dispersed in deionized water and mixed with silver nitrate. After the color changed, they were centrifuged and dried (Scheme 40).

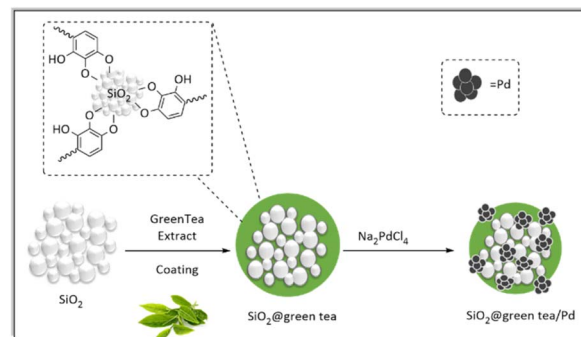
FT-IR and TGA confirmed the presence of green tea biomolecules in BSiO<sub>2</sub>. Color change/UV-Vis and XRD verified that catechins and polyphenols from green tea extract acted as reducing agents for Ag<sup>+</sup> to Ag<sup>0</sup>, forming Ag NPs. XPS, HRTEM, and EDS showed well-dispersed Ag NPs coated with extract molecules, providing stabilization and size control. After the identification, the catalytic activity of the Ag-BSiO<sub>2</sub> nanohybrids was investigated in the synthesis of dihydroquinoline derivatives *via* the reaction of 1-(2-aminophenyl)ethan-1-one and various aryl aldehydes (Scheme 41).

To perform the reaction under the best conditions, the effect of different solvents was first investigated under reflux conditions. Among the solvents including toluene, THF, acetonitrile, EtOH, dioxane, H<sub>2</sub>O and DMF, the best activity was observed in acetonitrile. When acetonitrile was used as a solvent at 60 °C for 6 hours, the desired product was obtained with a yield of 93%. Increasing the catalyst dose to 0.5 mol% led to the highest yield and adding more catalyst to the medium had no effect on the yield and reaction rate. No significant difference in yield or reaction time was observed among 2-chlorobenzaldehyde, 4-chlorobenzaldehyde, and 4-methoxybenzaldehyde, with yields in the range of 91–93% and reaction times between 6–7 h.

The recycled Ag-BSiO<sub>2</sub> nanohybrid was tested in 5 consecutive reactions to show its reusability, and even in the 5th cycle of the catalytic reaction, it showed the same effective reactivity as in the 1st cycle.

The Buchwald–Hartwig amination reaction allows for the generation of C(sp<sup>2</sup>)-N bonds through the Pd-catalyzed coupling of (hetero)aryl halides and pseudohalides with amines.<sup>110</sup> This reaction is an important method to do an essential transformation in organic synthesis, as the product is a key framework in numerous naturally occurring products, drugs, and other biologically active compounds.<sup>111</sup>

Veisi *et al.* reported the efficient synthesis of arylamines by Buchwald–Hartwig C–N cross-coupling reaction using a green



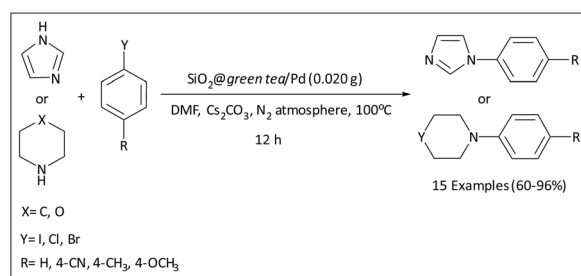
**Scheme 42** Green metric synthesis of the SiO<sub>2</sub>@green tea/Pd nanocomposite and its catalytic use in Buchwald–Hartwig C–N coupling.

tea extract catalyst formulated as SiO<sub>2</sub>@green tea/Pd nanocomposite.<sup>112</sup>

To prepare the catalyst, green tea leaves were collected from northern Iran and after washing with distilled water, they were extracted by boiling in deionized water and filtered to obtain a clear aqueous extract. In the next step, silica gel was dispersed in water and subjected to ultrasound. Then green tea extract was added to the mixture and after adding green tea extract, the mixture was stirred for 24 hours and the final product was separated and dried. In continue the SiO<sub>2</sub>@green tea nanocomposite was dispersed in water and Na<sub>2</sub>PdCl<sub>4</sub> was added to reduce palladium ions. Then after washing and drying the final product (SiO<sub>2</sub>@green tea/Pd) became ready for use (Scheme 42).

After preparation of the SiO<sub>2</sub>@green tea/Pd nanocomposite, SEM and TEM analysis revealed porous silica sheets with uniformly dispersed Pd NPs, indicating capping and stabilization by polyphenols and other biomolecules from green tea. EDX and ICP-AES confirmed Pd loading and attachment of C, N, O from the extract. XRD and XPS verified Pd<sup>2+</sup> reduction to Pd<sup>0</sup> and formation of a stable nanocomposite. Then its catalytic activity was studied in the Buchwald–Hartwig amination reaction between aryl halides and various amines using Cs<sub>2</sub>CO<sub>3</sub> as a base in dimethylformamide (DMF) solvent under N<sub>2</sub> atmosphere at 100 °C (Scheme 43).

The reactions were performed using 0.5 mol% of the catalyst, leading to desired derivatives in 12 hours. This approach enabled the synthesis of diverse arylamine derivatives through the coupling of substituted aryl halides with secondary amines,



**Scheme 43** N-Arylation of aryl halides *via* the Buchwald–Hartwig reaction catalyzed by the SiO<sub>2</sub>@green tea/Pd nanocomposite.



in yields ranging from 60 to 96%. Different substituents, such as  $\text{CH}_3$ ,  $\text{OCH}_3$ , and  $\text{CN}$ , on bromoarenes and iodoarenes showed high compatibility with this process, and there was no significant difference in the electron-withdrawing or electron-donating effects of the substituents. However, under these conditions, chloroarenes demonstrated lower reactivity compared to their bromo or iodo counterparts.

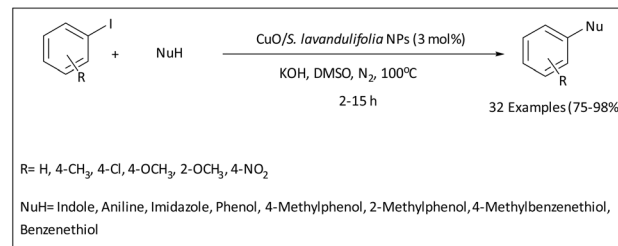
As the catalyst reusability is considered as an important feature of a catalyst, and in order to show this characteristic in the case of the introduced catalyst, the reaction of bromobenzene and morpholine was studied again under the optimized conditions. The obtained results confirmed that the catalyst is well able to be used up to six consecutive times without any significant change in its catalytic activity.

Cross-coupling reactions catalyzed by transition metals are currently one of the most widely used transformations in organic synthesis.<sup>113</sup> Products of cross-coupling reactions, especially heterocyclic coupling products, have very important biological and medicinal values and facilitate further drug development processes.

A novel nano-catalyst ( $\text{CuO/S. lavandulifolia}$  NPs) for the C-heteroatom (N, O, and S) cross-coupling with a green and convenient approach using the plant tea flower extract (*Stachys Lavandulifolia*) was synthesized and reported by Veisi and co-workers in 2021.<sup>114</sup>

To prepare the catalyst, first, fresh herbal tea (*Stachys Lavandulifolia*) flowers were washed, dried, and dispersed in Milli-Q water. Following heating, the extract was filtered through Whatman No. 1 filter paper and subsequently centrifuged. For  $\text{CuO}$  nanoparticle synthesis, the extract was combined with a 1 mM copper(II) acetate solution and heated. NPs formation was confirmed by the color change to dark brown, which is the result of surface plasmon resonance excitation. The precipitate was washed and dried leading to the preparation of the  $\text{CuO/S. lavandulifolia}$  NPs catalyst (Scheme 44). In continue, the synthesized  $\text{CuO}$  NPs were characterized (UV-Vis, FT-IR, FE-SEM, TEM, EDX, XRD, TGA), confirming  $\text{CuO}$  NP formation, uniform size, high crystallinity, and thermal stability, and demonstrating simultaneous reduction and capping/stabilization by flavonoids, polyphenols, and alkaloids from *Stachys lavandulifolia*.

After identification of the catalyst, the reaction model of iodobenzene with indole, phenol and thiophenol was screened in the presence of it. The best times and yields for the Ar-C-N/O/S mediated coupling reactions were obtained by heating the



Scheme 45 C-Heteroatom cross coupling reactions using  $\text{CuO}$  NPs as the catalyst.

reaction mixture in DMSO solvent, at 100 °C and in the presence of the  $\text{CuO/S. lavandulifolia}$  NP catalyst (3 mol%).

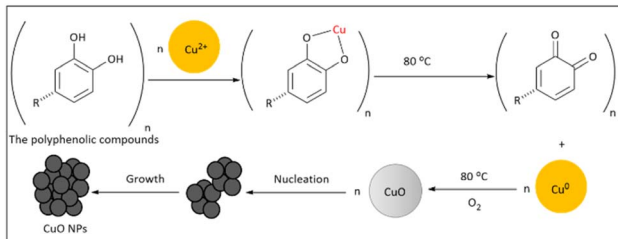
Under the selected conditions, various aryl and heteroaryl *N*-nucleophiles (indole, imidazole, and aniline), *O*-nucleophiles (substituted phenols), and *S*-nucleophiles (substituted thiophenols) reacted smoothly with aryl iodides bearing electron-donating or electron-withdrawing groups, affording products in 75–98% yields. Aniline reacted more rapidly with aryl iodides than indole or imidazole (Scheme 45). In this method the reported heterogeneous nanocatalyst was isolated, recycled and reused in 8 consecutive periods without significant change in its activity.

Acetylation stands as one of the most crucial reactions in organic synthesis. *O*-Acetylation of alcohols and phenols is a process that is not only useful for the protection of hydroxyl groups, but also helps to improve biological and pharmaceutical activities.<sup>115–117</sup>

In 2023,  $\text{Fe}_3\text{O}_4@\text{CLS/Ag}$  was synthesized as a novel nanocatalyst using green tea extract by Wang and co-workers.<sup>118</sup> The synthesized catalyst served a critical function in the *O*-acetylation reactions of alcohols and phenols by facilitating the reaction and improving efficiency.

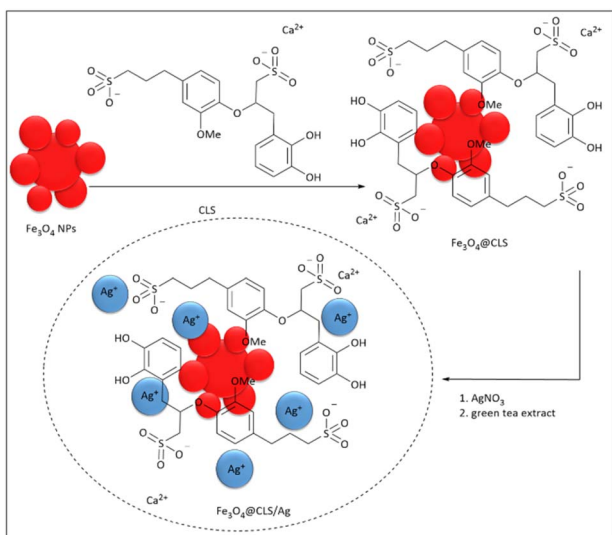
For the catalyst preparation, the  $\text{Fe}_3\text{O}_4$  nanoparticles were produced through simultaneous precipitation of  $\text{Fe}^{2+}$  and  $\text{Fe}^{3+}$  ions. Then an aqueous solution of calcium lingo-sulfonate (CLS) was prepared and the  $\text{Fe}_3\text{O}_4$  nanoparticles were added to it, and after stirring for 12 hours, the  $\text{Fe}_3\text{O}_4@\text{CLS}$  nanocomposite was obtained. To prepare green tea extract, 1 g of the green tea leaves was boiled in 100 mL of deionized water and strained. Then the  $\text{Fe}_3\text{O}_4@\text{CLS}$  nanocomposite was combined with  $\text{AgNO}_3$  solution and the green tea extract and after stirring for 2 hours, Ag ions were reduced to the silver nanoparticles. The completion of the reaction was evidenced by a color shift from pale yellow to dark brown. Subsequently, the  $\text{Fe}_3\text{O}_4@\text{CLS/Ag}$  nanocomposite was isolated and dried (Scheme 46).

The structural and physicochemical features of the  $\text{Fe}_3\text{O}_4@\text{CLS/Ag}$  nanocomposite were evaluated through several analytical techniques. SEM and TEM revealed spherical to quasi-spherical  $\text{Fe}_3\text{O}_4$  and Ag NPs with uniform dispersion, indicating capping and stabilization by CLS and green tea biomolecules. EDX/elemental mapping confirmed uniform Fe, Ag, C, and O distribution, while ICP-OES verified effective metal loading. VSM showed preserved paramagnetic properties despite surface coverage by green tea biomolecules and CLS.

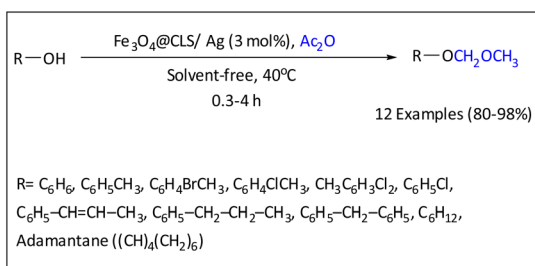


Scheme 44 Mechanistic investigation of  $\text{CuO}$  NPs biosynthesis mediated by *Stachys lavandulifolia* extract.





**Scheme 46** Biogenic synthesis of the  $\text{Fe}_3\text{O}_4@\text{CLS}/\text{Ag}$  nanocomposite and its application in the  $O$ -acetylation of alcohols and phenols.



**Scheme 47** O-Acylation of phenols with  $\text{Ac}_2\text{O}$  catalyzed by  $\text{Fe}_3\text{-O}_4@\text{CLS}/\text{Ag}$ .

The identified nanocomposite showed a very good potential in the promotion of *O*-acetylation with acetic anhydride under solvent-free conditions, affording yields in the range of 80–98% (Scheme 47).

As a probe reaction to optimize conditions such as temperature, catalyst loading and solvent, the reaction of phenol with acetic anhydride was selected. The reaction was tested in different media such as EtOH, MeOH,  $\text{CH}_2\text{Cl}_2$ , toluene,  $\text{CH}_3\text{CN}$  and water, with yields of 15–80%. Finally, the best yield was achieved without the use of a solvent at 40 °C and 3 mol% catalyst loading to achieve a yield of 96% within 1 h.

After the optimization studies, the *O*-acetylating ability of this method was tested on a variety of hydroxyl group-containing compounds including benzylic, allylic, primary, secondary, and tertiary alcohols. The results showed that benzyl alcohols with various halogen substituents were very compatible with the reaction conditions, with yields of 96–98% within 0.3 h. Under the selected conditions, unsaturated alcohols such as cinnamyl alcohol gave 85% yield in 2 h. On the other hand, various tertiary alcohols, which are esterically hindered and electron-rich (benzhydrol and adamantanol), were slow compared to the others, but eventually gave good yields in the

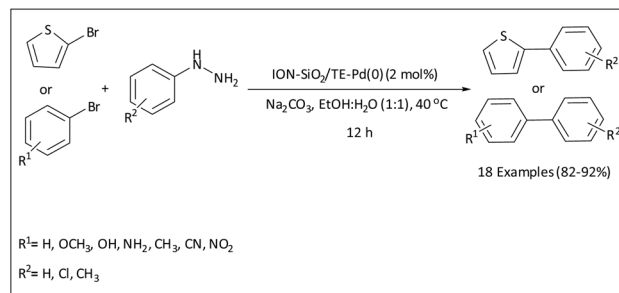
range of 80–90%. Also in this study, the prepared nanocatalyst can be recycled for 9 consecutive times without a noticeable decline in its activity.

Biaryl compounds are often found in many natural products, pharmaceuticals, and agrochemicals, as well as functional molecules.<sup>119</sup> Different approaches for the synthesis of biaryls include catalytic cross-coupling reactions such as Suzuki-Miyaura,<sup>120</sup> Stille<sup>121</sup> and Kumada.<sup>122</sup> However, these approaches suffer from drawbacks such as the use of expensive catalysts, toxicity of organic metals, and high amounts of the catalyst. According to the mentioned points, the preparation of heterogeneous catalysts in green conditions is very necessary for the construction of biaryl scaffolds with high efficiency.<sup>123-125</sup>

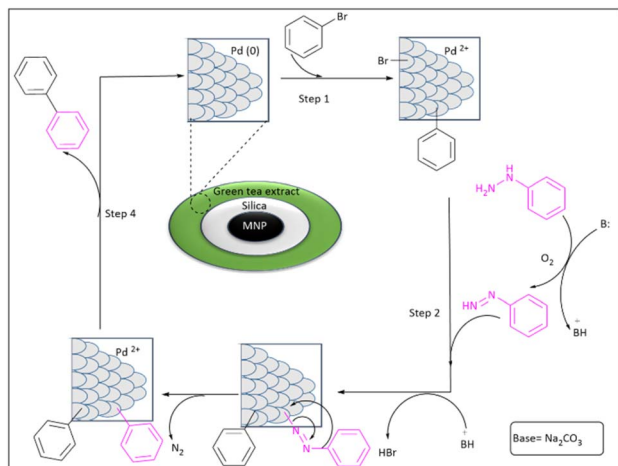
In 2023 Hegde *et al.* proposed ION-SiO<sub>2</sub>/TE-Pd(0) as an efficient nanocatalyst for the synthesis of biaryls.<sup>126</sup>

To prepare the catalyst, the tea extract was first prepared by boiling 10 grams of tea leaves in 100 mL of deionized water for 15 minutes, then filtered and stored at 4 °C. The iron oxide nanoparticles (IONPs) were synthesized by co-precipitation method and dried after washing with ethanol. The ION@SiO<sub>2</sub> nanocomposite was prepared by coating silica on IONPs in ethanol–water environment and adding tetraethyl orthosilicate and then dried. Finally, the ION@SiO<sub>2</sub>/TE-Pd(0) nanocatalyst was synthesized by adding Pd(OAc)<sub>2</sub> and tea extract to the ION@SiO<sub>2</sub> nanocomposite at 70 °C and after washing and drying.

During the characterization studies, FT-IR confirmed polyphenols, amino acids, and polysaccharides from tea extract (TE) can act as reducing and stabilizing agents; XRD revealed crystalline  $\text{Fe}_3\text{O}_4$  and Pd nanoparticles with uniform size; TGA indicated enhanced thermal stability due to TE coating; FE-SEM and HRTEM displayed spherical to quasi-spherical Pd nanoparticles preventing agglomeration and EDX/ICP-AES verified Pd loading, while VSM showed preserved paramagnetic properties despite surface coverage by TE, silica, and organic/polyphenolic layers. Then the catalytic activity of the ION-SiO<sub>2</sub>/TE-Pd(0) nanocatalyst was investigated for biaryl synthesis through the catalytic denitrogenation coupling reaction of aryl bromides and aryl hydrazines using 2 mol% ION-SiO<sub>2</sub>/TE-Pd(0) in the presence of Na<sub>2</sub>CO<sub>3</sub> in EtOH : H<sub>2</sub>O (1 : 1) at 40 °C (Scheme 48). The studied coupling reactions afforded the corresponding biaryls in 92% yields. It is worth noting that using this method



**Scheme 48** Denitrogenative coupling of aryl hydrazines with aryl halides by the ION-SiO<sub>2</sub>/TE-Pd(0) nanocatalyst.



**Scheme 49** Proposed mechanism for the denitrogenative bromobenzene and phenylhydrazine coupling by ION-SiO<sub>2</sub>/TE-Pd(0) nanocatalyst.

even 2-bromothiophene as a heteroaryl bromide couples with aryl hydrazines to give the desired products in 86–88% yield.

Reusability was tested to perform the stability of the catalyst in the reaction of phenylhydrazine and bromobenzene in the presence of the ION-SiO<sub>2</sub>/TE-Pd(0) nanocatalyst. The catalyst was reusable up to six cycles, with a 10% decrease in yield observed in the sixth run. The proposed mechanism for denitrogenation coupling of phenylhydrazine with bromobenzene catalyzed by ION-SiO<sub>2</sub>/TE-Pd(0) is shown in Scheme 49. This mechanism consists of 4 consecutive steps including: oxidative addition, migratory insertion, denitration, and reductive elimination.

### Multi-component reactions

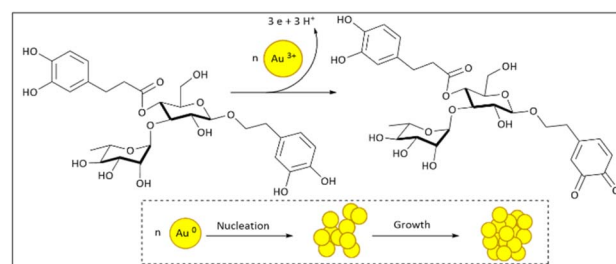
In response to growing environmental concerns, there has been an active movement toward the development of green chemical processes employing eco-friendly chemicals, reagents, solvents and catalysts. In this regard, selectivity, saving atoms, saving time, compatibility with the environment, cost-effectiveness and matching molecular complexity with experimental simplicity are considered as very important factors. Recently, multicomponent reactions based on the principles of green and sustainable chemistry have been widely used to prepare important organic molecules. A multi-component reaction (MCR) is a synthetic method in which three or more reactants react in a reaction vessel to form a new product.<sup>127–131</sup> Multi-component reactions are recognized as powerful strategies in the synthesis of complex organic compounds, drugs, and heterocyclic building blocks due to their high efficiency and simplicity of the process.<sup>132</sup> The characteristic features of these reactions are the maximum utilization of starting materials and the production of minimal by-products, which reduce the number of steps, eliminates the need for separation of intermediates, and increases the yield in a shorter time.<sup>133</sup> In addition, MCRs have attracted widespread attention in industrial and academic research due to their green chemistry principles, operational simplicity, atom economy, and high selectivity.<sup>134,135</sup>

Tea-mediated nanocatalysts have found widespread application in multi-component reactions. The efficiency of tea-based nanocatalysts is attributed to the polyphenols, flavonoids, and other biomolecules present in tea, which act as reducing and stabilizing agents. These compounds not only enable control over the shape, size, and dispersion of metal nanoparticles but also enhance the recyclability, stability, and substrate tolerance of the catalytic system. Accordingly, tea-mediated nanocatalysts are recognized as sustainable, efficient, and versatile catalytic systems for multicomponent organic syntheses.

Propargylamines are a class of versatile compounds which are able to use as building blocks in the synthesis of chemically related organic compounds.<sup>136</sup> They are also the main intermediates for the preparation of biological drugs and useful natural products. Some propargylamine derivatives are used against neurological disorders such as Parkinson's and Alzheimer's disease.<sup>137</sup> These compounds have been developed by various methods such as A<sup>3</sup>-coupling reaction (three-component coupling),<sup>138</sup> nucleophilic substitution,<sup>139</sup> reductive amination,<sup>136</sup> and Sonogashira coupling,<sup>140</sup> which of them A<sup>3</sup>-coupling is the most widely used due to its efficiency and ease of implementation.

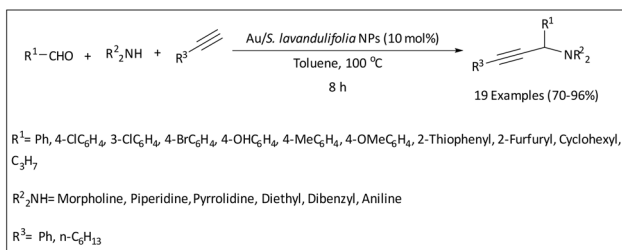
Veisi and co-workers reported an efficient heterogeneous catalyst formulated as Au/S. *lavandulifolia* NPs using herbal tea for the three-component reaction of amines, aldehydes and alkynes (coupling A<sup>3</sup>) in 2018.<sup>141</sup>

To prepare the Au/S. *lavandulifolia* NPs nanocatalyst, herbal tea collected from Zagros region (Iran), was cleaned, dehydrated, and used to prepare the *Stachys Lavandulifolia* extract. Tea was combined with Milli-Q water and heated. Then the extract was filtered and centrifuged. The *Stachys Lavandulifolia* extract was introduced into a 1 mM HAuCl<sub>4</sub> H<sub>2</sub>O aqueous solution (100 mL) at room temperature and stirred. The color of the solution turned to red within 2 hours and then the solutions containing nanoparticles were centrifuged and washed several times with deionized water and finally oven-dried (Scheme 50). Characterization by UV-Vis confirmed the rapid formation of Au NPs with increasing extract content, while FT-IR revealed polyphenolic groups responsible for reduction and stabilization. XRD and FFT confirmed the crystalline fcc structure, and EDS verified the purity of metallic gold. SEM, AFM, and HRTEM images showed spherical/triangular NPs with uniform distribution (20–30 nm), and TGA demonstrated good thermal stability due to organic capping from the extract.



**Scheme 50** Preparation of Au NPs using *Stachys lavandulifolia* extract.

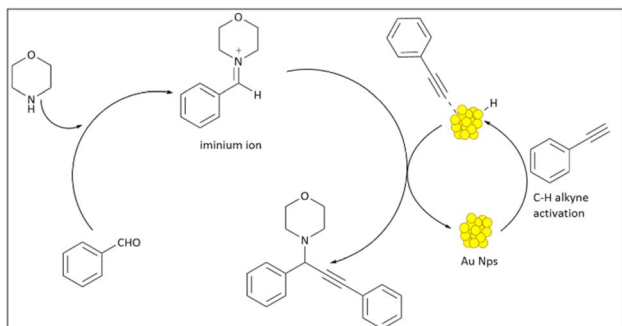




**Scheme 51** The  $A^3$ -coupling reaction in the presence of the Au/S. *lavandulifolia* NPs catalyst.

The catalytic power of the Au/S. *Lavandulifolia* NPs catalyst was investigated in the  $A^3$ -coupling reaction of aldehydes, amines and alkynes, leading to the formation of a diverse range of propargyl amines. In order to optimize the conditions, different types of solvents, temperatures, and the catalyst loading were tested on the reaction of benzaldehyde (1.0 mmol), morpholine (1 mmol), and phenylacetylene (1.2 mmol). Among the examined solvents (toluene,  $CH_2Cl_2$ , DMF, EtOH,  $H_2O$ ,  $CH_3CN$ , and neat condition) the best performance was observed in toluene solvent. Carrying out the reaction at 100 °C in toluene using 10 mol% catalyst resulted in the highest yield (92%). Further increase in the amounts of the catalyst had no effect on increasing the reaction yield (Scheme 51). In this study, the reaction yield is related to the type of the used aldehyde. According to the observed results, the behavior of aromatic aldehydes with  $-Cl$ ,  $-Br$ ,  $-OH$ ,  $-Me$  or  $-OMe$  functional groups can affect the  $A^3$ -coupling reaction. Aryl halides with electron-withdrawing groups can produce the corresponding products in excellent yields (95–96%), while the substitution of electron-rich groups on the benzene ring leads to a decrease in the catalyst performance and reaction efficiency (85–90%).

The recyclability of the Au/S. *Lavandulifolia* NPs catalyst was also examined for the reaction involving benzaldehyde, morpholine, and phenylacetylene. It was found that the catalyst could be reused for as many as seven cycles with no notable loss in its catalytic activity. The proposed mechanism of the  $A^3$ -coupling reaction under heating by the Au/S. *lavandulifolia* NPs catalyst is shown in Scheme 52. Based on this mechanism at the first step, the terminal alkyne is activated by the catalyst under heating to form the corresponding Au-alkylidene complex on



**Scheme 52** Probable mechanism for the  $A^3$ -coupling reaction using Au/S. *lavandulifolia* NPs.

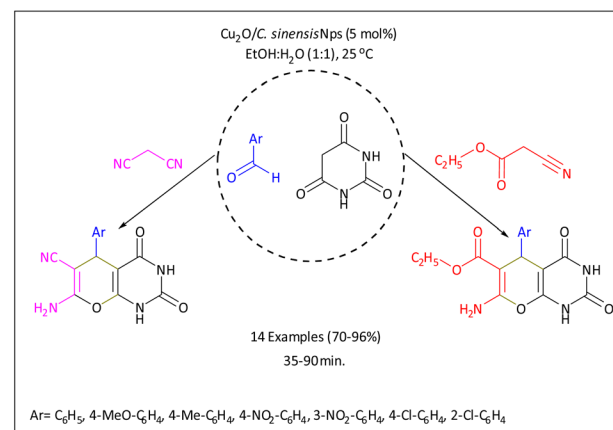
the nanoparticle surface. During, the next step, the Au-acetylidyne intermediate reacts with the iminium ion, generated from the aldehyde and amine at the reaction site, which leads to the formation of the desired propargylamine. In continue the Au/S. *lavandulifolia* NPs catalyst is reformed to be used in the subsequent cycles.

Pyrido[2,3-*d*]pyrimidines are quinazoline derivatives showing a wide range of biologically important activities, including antitumor, antibacterial, CNS depressant, anticonvulsant, antipyretic, analgesic, anticancer activities, and anti-proliferative.<sup>142–144</sup>

Because of this Dou *et al.* reported the preparation of the Cu<sub>2</sub>O/C. *sinensis* NPs nanocatalyst using *Camellia sinensis* leaf aqueous extract with a facile method and its use in promotion of the one-pot synthesis of pyrano[2,3-*d*]pyrimidines.<sup>145</sup>

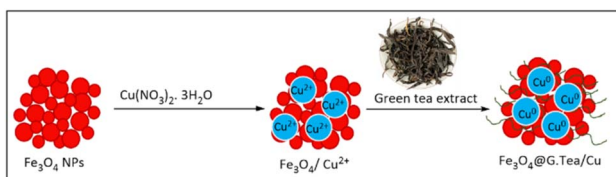
To prepare the Cu<sub>2</sub>O/C. *sinensis* NPs nanocatalyst, firstly, *Camellia sinensis* leaf extract was obtained using distilled water under microwave irradiation. In a typical synthetic method, NaOH and CuCl<sub>2</sub>·2H<sub>2</sub>O pellets were each dissolved in distilled water and mixed well, and then the *Camellia sinensis* leaf extract solution was added to them under vigorous stirring. The color change of the solution to brick red indicates the formation of the copper oxide nanoparticles (Cu<sub>2</sub>O NPs). The resulting solution was refluxed until a precipitate was formed. After that, the filter sediment was washed and dried to obtain a fine powder of the Cu<sub>2</sub>O nanoparticles. During the structural studies, XRD confirmed the crystalline Cu<sub>2</sub>O phase, while FT-IR identified hydroxyl groups and aromatic rings originating from *Camellia sinensis* polyphenols, which acted as reducing and stabilizing agents. TEM/FE-SEM revealed spherical, uniformly distributed nanoparticles, and EDX/elemental mapping verified the presence of Cu and O, with tea-derived biomolecules covering the surface and preventing agglomeration.

In continue, the catalytic activity of the Cu<sub>2</sub>O/C. *sinensis* NPs in the synthesis of pyrano[2,3-*d*]pyrimidines was investigated *via* a three-component one-pot condensation of aromatic aldehydes, barbituric acid and ethyl cyanoacetate/malononitrile at room temperature using 5 mol% catalyst in EtOH/H<sub>2</sub>O (1:1) media. The reaction proceeded well and all the products were



**Scheme 53** Synthesis of pyrano[2,3-*d*]pyrimidines catalyzed by the Cu<sub>2</sub>O/C. *sinensis* NPs.





**Scheme 54** Bio-inspired synthetic strategy for the synthesis of  $\text{Fe}_3\text{O}_4@\text{G.tea/Cu}$  nanocomposite over green tea extract.

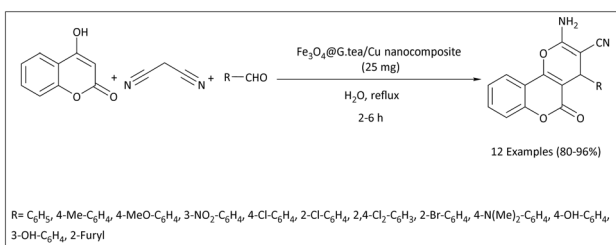
obtained in excellent yields ranging from 70 to 96% (Scheme 53).

The obtained results showed that the  $\text{Cu}_2\text{O}/\text{C sinensis}$  NPs nanocatalyst can be recycled for at least 10 consecutive times without significant change in its activity which indicates its considerable stability during the course of the reaction.

Chromenes are an important class of oxygen containing heterocycles with diverse biological properties. Among them, pyrano[3,2-c] chromene derivatives have received attention in recent years. This is because that these compounds are used in the scaffolding of the structure of important medicinal molecules that have a wide range of medicinal aspects such as antiviral, antitumor, sedative, antitumor, anti-HIV, antifertility, anticancer, antidepressant, antihypertensive, anticoagulant, antimicrobial, diuretic, and analgesic.<sup>146,147</sup>

In 2022, Xu *et al.* reported that the  $\text{Fe}_3\text{O}_4@\text{G.tea/Cu}$  nanocomposite as a heterogeneous reagent can promote the synthesis of pyrano[3,2-c]chromene derivatives with excellent efficiency.<sup>148</sup>

For the preparation of the catalyst, firstly dried green tea leaves were collected, washed and heated in water. After filtration, green tea extract was obtained. In the next step, the pre-synthesized  $\text{Fe}_3\text{O}_4$  NPs were sonicated in deionized water and then  $\text{CuNO}_3$  was mixed with dispersion. Finally, green tea extract as a reducer was added to it to obtain the copper nanoparticles. The  $\text{Fe}_3\text{O}_4@\text{G.tea/Cu}$  nanocomposite was magnetically separated and then washed with DI water and dried (Scheme 54). FT-IR confirmed polyphenols and hydroxyl groups from green tea, acting as reducing and stabilizing agents for Cu NPs. TEM/SEM showed quasi-spherical, uniformly distributed Cu and  $\text{Fe}_3\text{O}_4$  nanoparticles, while EDX/elemental mapping confirmed Fe, Cu, C, and O with uniform polyphenol coverage, stabilizing Cu NPs and preventing agglomeration. XRD confirmed crystalline phases, and VSM/ICP-OES



**Scheme 55** Synthesis of pyrano[3,2-c]chromene derivatives using the  $\text{Fe}_3\text{O}_4@\text{G.tea/Cu}$  as nanocatalyst.

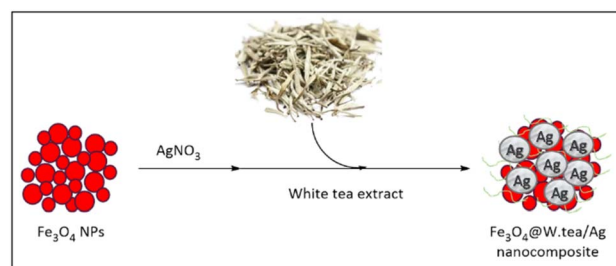
indicated preserved magnetic properties and stable Cu loading due to the green tea coating.

After the identification studies, the catalytic properties of the catalyst was investigated in the synthesis of pyrano[3,2-c] chromenes. To optimize the conditions, different solvents, catalyst amounts and temperatures were tested. Among the various solvents such as EtOH, *n*-hexane,  $\text{CH}_3\text{Cl}$ ,  $\text{CH}_2\text{Cl}_2$ , toluene, acetonitrile and water at the respective reflux temperature, the best performance in terms of the reaction yield (96%) and time (2 h) was observed in water. After examining different amounts, it was found that 25 mg of the catalyst had the best performance and increasing it beyond this amount had no effect on the reaction time and yield. Thus, the reaction to prepare 2-amino-4-aryl-4,5-dihydropyran[3,2-c]chromene-3-carbonitrile derivatives was carried out under reflux conditions in water, using 25 mg of the catalyst by employing a wide range of aromatic and heteroaromatic aldehydes with variable functional groups. All substrates, regardless of the electron-withdrawing/donating nature of the substituents produced the corresponding products in excellent yields (80–96%). No detectable effect of the location of the functional groups on the ring was observed (Scheme 55).

In this study the reusability of the  $\text{Fe}_3\text{O}_4@\text{G.tea/Cu}$  nanocatalyst was also investigated. The nanocatalyst was reused 8 times in a row without significant reduction in its activity.

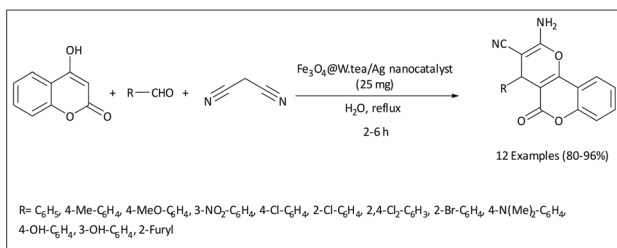
In the other study, in 2022 the  $\text{Fe}_3\text{O}_4@\text{W.tea/Ag}$  nanocomposite catalyst was prepared using white tea extract *via* an environmentally friendly and low-cost method for the synthesis of pyrano[3,2-c]chromenes by Hou and co-workers.<sup>149</sup>

For the synthesis of the catalyst, at first, the research group completely washed the dried white tea leaves with deionized water and then heated, and after filtering, the white tea extract was obtained. In the next step,  $\text{Fe}_3\text{O}_4$ NPs was synthesized by the coprecipitation method. The dried and activated nanoparticles were dispersed in deionized water. Then,  $\text{AgNO}_3$  was added to the mixture and stirred for 30 minutes to stabilize Ag ions on  $\text{Fe}_3\text{O}_4$ NPs. Then, white tea extract was added as a green regenerator and silver nanoparticles stabilizer. The  $\text{Fe}_3\text{O}_4@\text{W.tea/Ag}$  nanocomposite was finally separated using a magnet, washed with deionized water and dried (Scheme 56). The results obtained from the FT-IR analysis confirmed the presence of polyphenols, catechins, flavonoids, and other bioactive compounds from white tea, responsible for reducing and stabilizing Ag NPs. TEM/SEM showed spherical 15–20 nm  $\text{Fe}_3\text{O}_4$



**Scheme 56** Green synthesis of the  $\text{Fe}_3\text{O}_4@\text{W.tea/Ag}$  nanocomposites using white tea extract.





**Scheme 57** Synthesis of the pyrano[3,2-c]chromene derivatives in the presence of  $\text{Fe}_3\text{O}_4@\text{W.tea/Ag}$  as nanocatalyst.

and Ag nanoparticles with uniform distribution and minimal agglomeration, stabilized by tea biomolecules. VSM and ICP-OES indicated that the white tea coating preserved the magnetic properties and ensured stable Ag loading (0.13 mmol g<sup>-1</sup>).

After precise identification of the  $\text{Fe}_3\text{O}_4@\text{W.tea/Ag}$  nanocomposite, it was used as a catalyst in three-component condensation of 4-hydroxycoumarin, malononitrile, and aromatic and heteroaromatic aldehydes to synthesize 2-amino-4-aryl-4,5-dihydropyrano[3,2-c]chromene-3-carbonitrile derivatives (Scheme 57).

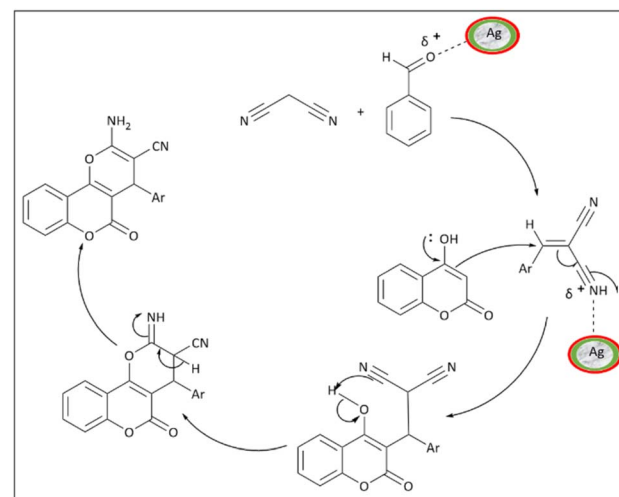
To optimize the reaction conditions different solvents such as EtOH, *n*-hexane,  $\text{CH}_3\text{Cl}$ ,  $\text{CH}_2\text{Cl}_2$ , toluene, acetonitrile and water were tested at reflux temperature and the best results were obtained in water. Then different amounts of the catalyst were loaded to find out the best results. Using 25 mg of the catalyst in 2 hours resulted in 96% yield of the requested product. Using higher amounts of the catalyst did not make difference in the obtained products yield. In continue a various range of aromatic and heteroaromatic aldehydes with electron withdrawing/donating groups were used under the same conditions. All the products were obtained with excellent yields ranging from 80 to 96%, with no visible effect of the nature of substituted groups on the product yields. There was no marked effect on the geometry of the functional groups. This catalyst was recycled for 8 consecutive times without a significant decrease in its activity.

The proposed mechanism for the synthesis of 2-amino-4-aryl-4,5-dihydropyrano[3,2-c]chromene-3-carbonitrile derivatives using the  $\text{Fe}_3\text{O}_4@\text{W.tea/Ag}$  nanocatalyst is shown in Scheme 58.

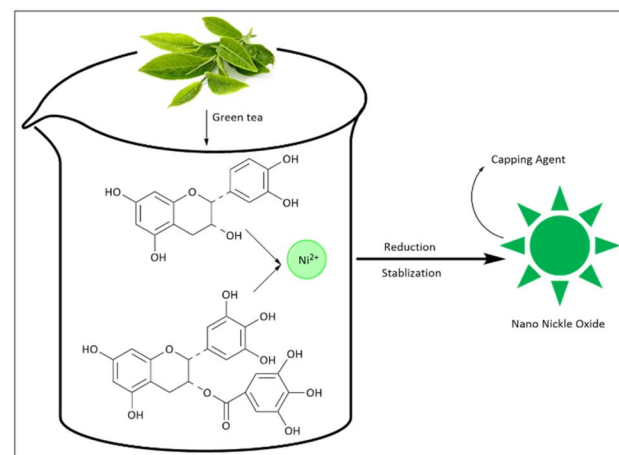
3,4-Dihydropyrimidin-2(1*H*)-one compounds (DHPMs) are often prepared from the Biginelli and *N*-alkylation reactions. DHPMs are developing in medicinal chemistry and have various biological activities including antitumor, antiviral, anti-leishmania, antibacterial, antifungal, anti-epileptic, antidiabetic, anti-malarial, and anti-inflammatory.<sup>150</sup>

In 2022 using a green method, Khashaei and co-workers synthesized NiO NPs and used it for the first time in the Biginelli reaction to receive to higher performance in the synthesis of 3,4-dihydropyrimidin 2(1*H*)-ones (DHPMs).<sup>151</sup>

To prepare the catalyst, first of all, the plants [Orange blossom, Yarrow, Hibiscus tea, Green tea, Rosemary and/or Barberry] were dried and turned into powder. Then the powders were poured with distilled water under stirring at



**Scheme 58** Probable mechanism for the synthesis of 2-amino-4-aryl-4,5-dihydropyrano[3,2-c]chromene-3-carbonitrile.

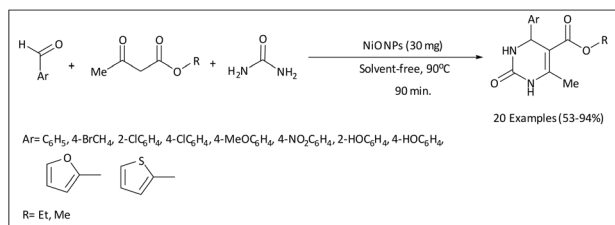


**Scheme 59** Schematic of the biosynthetic process of NiO nanoparticles using green tea extract.

a temperature of 70 °C. Then, the extracts were stored at 4 °C after filtration. For the green synthesis of NiO NPs,  $\text{Ni}(\text{NO}_3)_2 \cdot 6\text{H}_2\text{O}$  was dissolved in deionized water and then mixed with each of the natural surfactants, while the pH was adjusted with an ammonia solution. After stirring and sonication, the mixture was heated in an autoclave for 24 hours at a temperature of 80 °C. The product was washed and dried, and finally, to remove organic components, they were placed in an oven at a temperature of 410 °C for 10 h (Scheme 59).

In case of this catalyst, XRD confirmed the cubic structure with extract-controlled crystal size. FE-SEM showed porous 20–60 nm particles with uniform distribution. FT-IR confirmed adsorption of active extract compounds (OH, C–O) on NiO, enhancing nanoparticle stability, while UV-Vis revealed direct band gap energies (2.30–2.70 eV) influenced by extracts, reflecting controlled particle size and improved optical properties. After confirming the structure of the synthesized





Scheme 60 Schematic representation of the synthesis of 3,4-dihydropyrimidin 2(1H)-ones (DHPMs).

nanocatalysts (NiO NPs) the reaction conditions for the synthesis of DHPMs were optimized and then it was used to prepare 3,4-dihydropyrimidin-2(1H)-one derivatives from the 3-component reaction of aryl aldehydes, ethyl acetoacetate/methyl acetoacetate, and urea (Scheme 60). For this purpose the reaction was carried out at 90 °C under solvent-free conditions using 30 mg of the catalyst (0.04 mol%). The formation of DHPMs was facilitated by the activation of the reactants through the Lewis acidic ( $\text{Ni}^{2+}$ ) and basic sites of the NiO NPs.

All the catalysts used in these processes are recyclable and reusable, and they can be repeatedly recycled up to the fourth step of the reaction without a decrease in the performance or loss of efficiency.

The proposed reaction mechanism for the synthesis of DHPMs using the prepared NiO nanocatalysts is presented in Scheme 61.

### Miscellaneous reactions

As we have previously mentioned, tea-derived nanocatalysts have demonstrated high performance in a variety of organic transformations, including carbénoid etherification, selective hydrogenation, and phenol polymerization. The bioactive

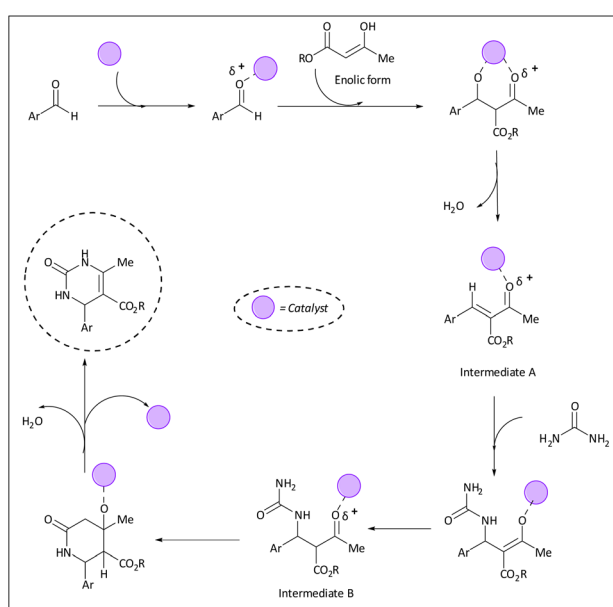
compounds present in tea, such as polyphenols, catechins, and flavonoids, naturally act as reducing and stabilizing agents, promoting the formation of metal nanoparticles with controlled size, uniform morphology, and high surface activity. These active components prevent nanoparticle aggregation and oxidation, significantly enhancing their stability and catalytic efficiency. Thanks to these properties, tea-derived nanocatalysts enable reactions under mild, eco-friendly conditions with high selectivity, broad substrate scope, and easy recyclability, while maintaining robust and reliable performance even under relatively harsh reaction conditions.

Carbene and carbénoids are very active intermediates in organic chemistry, which enable various transformations.<sup>152</sup> Carbénoids are usually obtained from diazo compounds and catalytic amounts of an intermediate metal such as Fe, Cu, Pd, Pt, Ni, Rh, Ru, Pd, Ag and Au.<sup>153</sup>

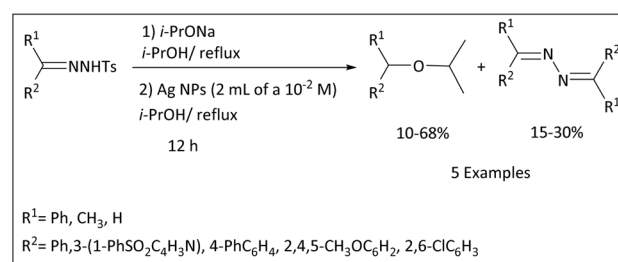
In 2012, Garcia and co-workers investigated the carbénoid etherification reaction of tosylhydrazones using silver nanoparticles as the catalyst prepared in the media of the green tea extract (*Camellia sinensis*).<sup>154</sup>

For this purpose, a green tea bag, containing 1.5 g of the dried herb, was boiled in 100 mL of 2-propanol for 1 min. Then the obtained extract was filtered. In the next step, the extract was added to a solution of  $\text{AgNO}_3$  (3–10 M) in 2-propanol. The reaction mixture was stirred at room temperature for 24 hours, leading to the formation of Ag NPs.

TEM analysis showed uniform, spherical Ag nanoparticles and well-separated ~5 nm Fe–Cu nanoparticles. Green tea extract acted as a natural reducing and stabilizing agent, preventing agglomeration and enhancing particle stability and surface activity, supporting higher catalytic efficiency. In continue, Ag NPs was used as a catalyst in the carbénoid etherification reaction of sodium salts of *p*-toluenesulfonylhydrazones in *i*-PrOH under reflux temperature (Scheme 62). This reaction led to the production of two major products, isopropyl ether and azine. The yields of these products varied depending on the type of tosylhydrazone used. The highest yield of isopropyl ether (68%) was obtained for the compound with the  $R^2 = 2,6\text{-ClC}_6\text{H}_3$  group, while for the compounds with the  $R^2 = 2,4,5\text{-CH}_3\text{OC}_6\text{H}_2$  group, the yield of ether decreased (10%) and the yield of azine increased (30%). The compound with the  $R^2 = 4\text{-PhC}_6\text{H}_4$  group had a higher yield of ether (67%) than that of azine (15%). These results indicate that the steric substituents in the  $R^2$  group have a direct effect on the yield of the products.

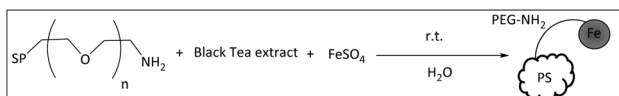


Scheme 61 Possible mechanistic pathway for the synthesis of DHPMs in the Biginelli reaction using the prepared catalysts.



Scheme 62 Carbenoid insertions using silver nanoparticles.



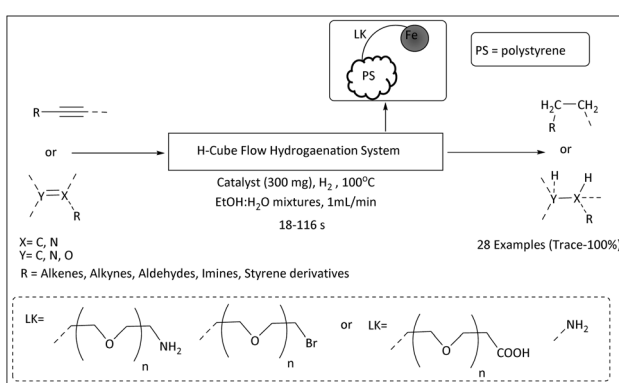
Scheme 63 Reduction of  $\text{FeSO}_4$  using black tea as a reducer.

Hydrogenation is a chemical process in which hydrogen molecules are incorporated into unsaturated compounds, usually in the presence of a catalyst, to generate saturated compounds.<sup>155</sup> This conversion reaction finds important uses in diverse industries including food manufacturing, petrochemicals, and pharmaceuticals.<sup>156</sup>

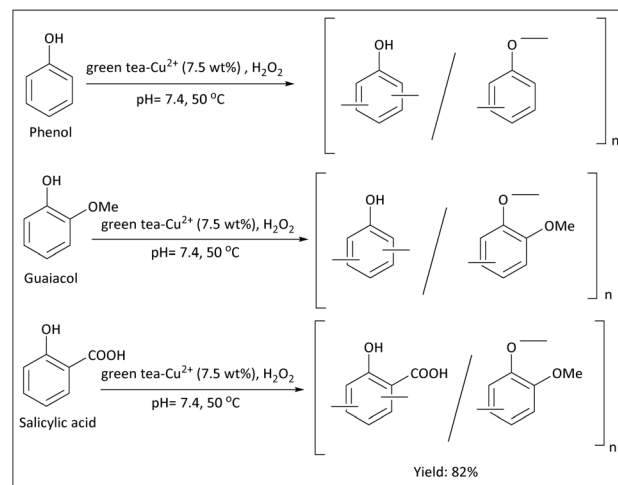
Although precious metal catalysts such as groups 9 and 10 metals are widely used in these reactions, due to high cost and environmental concerns, efforts to replace them with cheaper and non-toxic metals such as iron have increased.<sup>157</sup> In a report in 2013, Hudson *et al.* proposed iron nanoparticles stabilized with amphiphilic polymer ( $\text{FeNP@PS-(PEG)-NH}_2$ ) as an efficient and environmentally friendly catalyst for the hydrogenation of both alkenes and alkynes along with imines and aromatic ketones.<sup>158</sup> Synthesis of  $\text{FeNP@PS-(PEG)-NH}_2$  using black tea as a reducing agent was done according to the following method. Firstly, the Red Label black tea was steeped and introduced into a solution comprising amine-terminated polystyrene/polyethylene glycol beads,  $\text{FeSO}_4$ , and water. Subsequently, the mixture was agitated for 24 hours, after which the polymer was separated by filtration and gathered (Scheme 63).

TEM showed well-dispersed  $\sim 5$  nm  $\text{Fe}(0)$  nanoparticles stabilized by black tea polyphenols, preventing agglomeration, while ICP confirmed that Fe loading was  $\sim 5$  times lower than thermal methods due to the mild green reduction, yet nanoparticles remained stable and catalytically active.

The Fe NPs catalyst supported on amphiphilic polymer showed wide applications in the selective hydrogenation of various compounds including alkenes, alkynes, aromatic imines and aldehydes (Scheme 64). One of the outstanding features of this system is maintaining chemical selectivity (87–100%), such that functional groups such as aliphatic amines and aldehydes, ketones, esters, nitro and aryl halides remain un-affected.



Scheme 64 Schematic hydrogenation reactions undertaken with polymer supported iron nanoparticles, under flow conditions.

Scheme 65 Polymerization of phenol derivatives by the green tea- $\text{Cu}^{2+}$  nanobiocatalyst and  $\text{H}_2\text{O}_2$ , and the possible polymeric structures.

The polymerization of phenols is of great importance from the point of view of medicine and industry and has wide applications. Among the most important medicinal and industrial features of phenol polymerization are: antibacterial and antioxidant properties, biocompatibility and biodegradability, chemical and thermal resistance, and electrical insulation.<sup>159,160</sup>

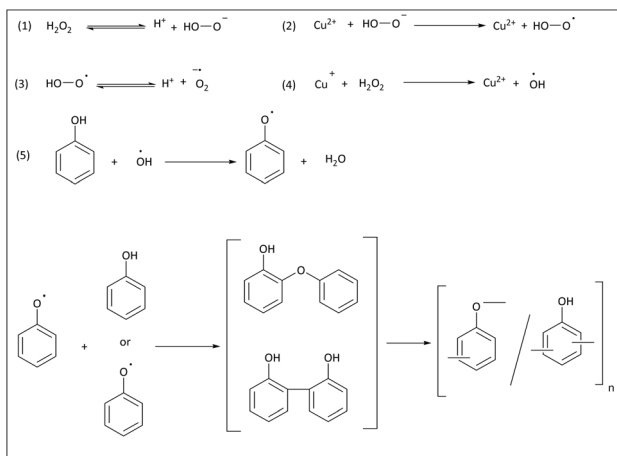
Because of this a green tea- $\text{Cu}^{2+}$  nanobiocatalyst was prepared through an environmentally friendly method for phenol polymerization by Kalayci and co-workers in 2024.<sup>161</sup>

At first, to prepare the green tea- $\text{Cu}^{2+}$  nanoflowers, powdered dry green tea was soaked in distilled water at 40 °C for one day, and then the extract was filtered and dried. The dry extract was stored in a refrigerator at 4 °C and used for the synthesis of nanobiocatalyst. The green tea extract was added to a solution of phosphate-buffered saline (PBS) (10 mM) and 0.8 mM  $\text{CuSO}_4 \cdot 5\text{H}_2\text{O}$ , the mixture was vortexed and incubated for 3 days at 4 °C. The resulting light blue precipitate was separated and washed by centrifugation. Finally, the deposit was kept in a dry oven and kept in a refrigerator at a temperature of 4 °C for the polymerization test.

SEM showed green tea- $\text{Cu}^{2+}$  nanobiocatalyst with uniform size distribution, while EDX confirmed the presence of Cu, and FT-IR indicated surface adsorption of green tea polyphenols, which stabilized the nanostructures and enhanced their catalytic activity. The polymerization of phenol and its derivatives (guaiacol and salicylic acid) was catalyzed by the green tea- $\text{Cu}^{2+}$  nanobiocatalyst using  $\text{H}_2\text{O}_2$ , and the obtained polymers showed a yield of 82% and excellent thermal stability with  $T_{50}$  of 624 °C and a molecular weight of 285 000 Da (Scheme 65).

The proposed mechanism for the polymerization of phenol promoted by the green tea- $\text{Cu}^{2+}$  nanobiocatalyst is shown in Scheme 66. According to this mechanism,  $\text{Cu}^{2+}$  ions are reduced to  $\text{Cu}^+$  in the presence of  $\text{H}_2\text{O}_2$ .  $\text{Cu}^+$  reacts with  $\text{H}_2\text{O}_2$  to produce hydroxyl radicals ( $\text{HO}^\cdot$ ). The hydroxyl radicals react with phenol molecules to form phenoxy radicals propagating polymerization through CC and CO pairs with phenol monomers.





Scheme 66 The polymerization mechanism of phenol.

## Critical evaluation and outlook

Tea-derived catalysts have emerged in recent years as promising materials in various organic reactions. These materials, benefiting from bioactive compounds found in different types

of tea, have demonstrated desirable features such as high stability, biocompatibility, and efficient catalytic performance. However, a critical evaluation of existing studies reveals that there are still serious challenges and limitations on the path toward industrial development and application of these catalysts.

Firstly, although most reported tea-based catalysts exhibit excellent recyclability and catalytic activity, they have generally been synthesized and tested only at the laboratory scale. The lack of industrial-scale reproduction methods and the absence of standardized synthesis protocols represent major barriers to commercialization. Furthermore, selectivity in complex reaction media—especially in the synthesis of pharmaceuticals or sensitive compounds—has not yet been thoroughly investigated.

Another significant challenge lies in the intrinsic variability of the chemical composition of different tea types. Variations in the type and quantity of polyphenols and other bioactive components may result in inconsistent catalytic behavior. In this regard, developing protocols for extract standardization or

Table 1 Review of characteristics, applications, and benefits of catalysts derived from various types of tea in catalytic processes

Tea type	Key reaction type	Avg. Recyclability	Characterization techniques	Advantages	Challenges	[Ref.]
Green tea	• Reduction	4–9 cycles	UV-Vis, FT-IR, XRD, XPS, TEM, TGA, FESEM, BET, HRTEM, ICP, SEM, EDS, VSM, elemental mapping, ICP-OES, FESEM, EDX	• Green and eco-friendly synthesis	• Optimization of synthesis conditions	55,60,61,65,67,
	• Coupling			• High catalytic efficiency	• Separation and purification	86,109,112,
	• MCR			• Stability and reusability	• Limitations in scalability	118,148,151,161 and 162
Black tea	• Reduction	4–9 cycles	UV-Vis, FT-IR, FESEM, EDX, XRD, TGA, TEM, SEM, XPS, ICP	• Versatility in catalyst design	• Extended reaction times	63,66 and 158
	• Coupling			• Green and eco-friendly synthesis	• Reaction limitations	
	• Hydrogenation			• High efficiency		
White tea	• Heterocyclic synthesis	4–8 cycles	FT-IR, XRD, SEM, EDX, TEM, VSM, ICP-AES	• Excellent stability	• Selective activity	
				• High stability	• Reaction condition optimization	100,105 and 149
				• Recyclability	• Replacement of toxic solvents	
Hibiscus tea	• Reduction	4–5 cycles	UV-Vis, TEM, XRD, FTIR, SEM, EDX	• Green synthesis	• Simplification of synthesis steps	
	• Biginelli			• Mild reaction conditions	• Complex synthesis process	53,88 and 151
	• Coupling			• High catalytic activity	• Separation process optimization	
Fenugreek tea	• Reduction	5 cycles	UV-Vis, SEM, SAED, FT-IR, XRD, TEM, XPS	• Excellent recyclability	• High energy consumption	64 and 89
	• Coupling			• Green synthesis	• Reaction condition optimization	
Herbal tea extract	• Reduction	7–9 cycles	FESEM, HRTEM, EDS, VSM, XRD, XPS, FT-IR, ICP, TEM, WDX, UV-Vis, AFM, TGA	• High selectivity	• Purification complexities	54,62,80,114 and 141
	• Coupling			• High recyclability	• Energy-intensive steps in synthesis	
	• MCR			• High catalytic efficiency	• High catalyst loading	
Yerba mate	• Coupling	3 cycles	ICP, FT-IR, FESEM, EDS, TEM, XPS, VSM	• Green and sustainable synthesis	• Limited recyclability	163
				• High efficiency for aryl iodides	• Longer reaction times for aryl bromides	





Table 2 Summary of tea-derived catalysts and their catalytic performance in organic transformations

Tea type	Catalyst composition	Metal salt	Reaction type	Substrate(s)	Reaction conditions	Yield/conversion (%)	[Ref.]
Green tea	Ag-TPG nanohybrid	AgNO <sub>3</sub>	Reduction	4-Nitrophenol	Cat. (0.5 mg mL <sup>-1</sup> ), NaBH <sub>4</sub> , H <sub>2</sub> O, N <sub>2</sub> , 12 min	100%	60
	γ-Fe <sub>2</sub> O <sub>3</sub> tubes decorated with Au NPs	HAuCl <sub>4</sub>	Reduction	4-Nitrophenol	Cat. (1.6 wt%), NaBH <sub>4</sub> , 4 min	89.62%	55
Ag-TPND		AgNO <sub>3</sub>	Reduction	4-Nitrophenol	Cat. (2 mL of 0.2 mg mL <sup>-1</sup> ), NaBH <sub>4</sub> , H <sub>2</sub> O, 16 min	92.1%	61
Fe <sub>3</sub> O <sub>4</sub> @GTE/Ag-NPs	AgNO <sub>3</sub> /Fe <sub>3</sub> O <sub>4</sub>	PdCl <sub>2</sub>	Reduction	4-Nitrophenol	Cat. (2 mg), NaBH <sub>4</sub> , H <sub>2</sub> O, r.t.	100%	65
Pd-NPs@G.Tea			Reduction	Nitro aromatics	Cat. (4 mg), NaBH <sub>4</sub> , EtOH:	90-96%	67
Pd/Fe <sub>3</sub> O <sub>4</sub> NPs	Na <sub>2</sub> PdCl <sub>4</sub>		Suzuki-Miyaura coupling	Aryl halide + phenyl boronic acid	H <sub>2</sub> O (1 : 1), 50 °C, 1-2 h		
			Suzuki-Miyaura coupling	Aryl halide + phenyl boronic acid	Cat. (2 mg), K <sub>2</sub> CO <sub>3</sub> , EtOH:	60-96%	
Ag-BSiO <sub>2</sub>	AgNO <sub>3</sub>			Aryl halide + phenyl boronic acid	H <sub>2</sub> O (1 : 1), 50 °C, 0.1-12 h		
					Cat. (35 mg), K <sub>2</sub> CO <sub>3</sub> , EtOH: H <sub>2</sub> O (1 : 1), 40 °C, 5-120 min	45-98%	86
SiO <sub>2</sub> @green tea/Pd nanocomposite	Na <sub>2</sub> PdCl <sub>4</sub>		Cyclization/Synthesis of dihydroquinolines	1-(2-aminophenyl)ethan-1-one + aryl aldehydes	Cat. (0.5 mol%), acetonitrile, 60 °C, 6-7 h	91-93%	109
Fe <sub>3</sub> O <sub>4</sub> @CLS/Ag	Fe <sup>2+</sup> /Fe <sup>3+</sup> salts (for Fe <sub>3</sub> O <sub>4</sub> )/AgNO <sub>3</sub>	Cu(NO <sub>3</sub> ) <sub>2</sub>	Batchwald-Hartwig C-N cross-coupling/O-acytlation	Aryl halides + amines	Cat. (0.020 g), DMF, Cs <sub>2</sub> CO <sub>3</sub> , N <sub>2</sub> , 100 °C, 12 h	60-96%	112
Fe <sub>3</sub> O <sub>4</sub> @G.tea/Cu nanocomposite			One-pot three-component condensation (MCR)	Alcohols + Ac <sub>2</sub> O	Cat. (3 mol%), Ac <sub>2</sub> O, solvent-free, 40 °C, 0.3-4 h	80-98%	118
NiO NPs	Ni(NO <sub>3</sub> ) <sub>2</sub> 6H <sub>2</sub> O		Biginelli three-component condensation	Aromatic/heteroaromatic aldehydes + malononitrile + 4-hydroxycoumarin	Cat. (25 mg), H <sub>2</sub> O, reflux, 2-6 h	80-96%	148
Ag NPs	AgNO <sub>3</sub>		Carbenoid etherification	Aryl aldehydes + methyl acetooacetate + urea	Cat. (25 mg), solvent-free, 90 °C, 90 min	53-94%	151
Green tea-Cu <sup>2+</sup> nanobiocatalyst	CuSO <sub>4</sub> ·5H <sub>2</sub> O		Polymerization	Tosylhydrazones	Cat. (2 mL), <i>i</i> -Pr <sub>2</sub> NO/ <i>i</i> -PrOH, reflux, 12 h	10-68% (isopropyl ethers)/15-30% (azines)	162
Pd@B.tea-NPs	PdCl <sub>2</sub>		Reduction				
Black tea			Suzuki-Miyaura coupling	Phenol, guaiacol, salicylic acid	Cat. (7.5 wt%), H <sub>2</sub> O <sub>2</sub> , pH = 7.4, 50 °C	82%	161
				4-Nitrophenol	Cat. (2 mg), NaBH <sub>4</sub> , H <sub>2</sub> O, r.t., 1 : 20 min	100%	63
Au-NPs	HAuCl <sub>4</sub> ·3H <sub>2</sub> O		Reduction	Aryl halide + aryl boronic acid	Cat. (0.006 g), K <sub>2</sub> CO <sub>3</sub> , EtOH: H <sub>2</sub> O (1 : 1), 60 °C, 0.16-12 h	65-98%	66
FeNP@PS-(PEG)-NH <sub>2</sub>	FeSO <sub>4</sub>		Hydrogenation	Nitro aromatics	Cat. (0.5 mL), NaBH <sub>4</sub> , H <sub>2</sub> O, r.t., 8 min	15-80%	158
				Alkenes, alkynes, aldehydes, imines	Cat. (300 mg), H <sub>2</sub> , 100 °C, EtOH: H <sub>2</sub> O, 13-116 s	Trace-100%	

Table 2 (Contd.)

Tea type	Catalyst composition	Metal salt	Reaction type	Substrate(s)	Reaction conditions	Yield/conversion (%)	[Ref.]
White tea	Wt- $\text{Fe}_3\text{O}_4$ MNPs	$\text{FeCl}_3 \cdot 6\text{H}_2\text{O}/\text{FeCl}_2 \cdot 4\text{H}_2\text{O}$	One-pot condensation/ Cyclization	<i>o</i> -Phenylenediamine + 4-chlorobenzaldehyde	Cat. (6 mol%), acetonitrile, 80 °C, 120 min	95%	100
	Pd@nanocat	PdCl <sub>2</sub>	Cross-coupling (diaryl ether formation)	Iodobenzene + phenol	Cat. (6 mol%), $\text{K}_3\text{PO}_4$ , DMSO, 120 °C, 7 h	94%	105
	$\text{Fe}_3\text{O}_4$ @W-tea/Ag nanocomposites	$\text{AgNO}_3$	One-pot three-component condensation (MCR)	Aromatic/heteroaromatic aldehydes + malononitrile + 4-hydroxycoumarin	Cat. (25 mg), $\text{H}_2\text{O}$ , reflux, 2–6 h	80–96%	149
Hibiscus tea	Ag-NPs	$\text{AgNO}_3$	Reduction	4-Nitrophenol	Cat. (100 $\mu\text{l}$ ), $\text{NaBH}_4$ , $\text{H}_2\text{O}$	—	53
	Pd NPs@ <i>Hibiscus sahdariffa</i> L.	PdCl <sub>2</sub>	Suzuki–Miyaura coupling	Aryl halide + phenyl boronic acid	Cat. (5 mg), $\text{K}_2\text{CO}_3$ , EtOH: $\text{H}_2\text{O}$ (1:1), 25 °C, 2–24 h	45–95%	88
Fenugreek tea	Pd-NPs@FT	PdCl <sub>2</sub>	Reduction	4-Nitrophenol	Cat. (1 mg $\text{mL}^{-1}$ ), $\text{NaBH}_4$ , $\text{H}_2\text{O}$ , 1 min	—	64
	PdPt	PdCl <sub>2</sub> /PtCl <sub>2</sub>	Suzuki–Miyaura coupling	Bromobenzene + phenyl boronic acid	PEG/Cat. (0.005 mmol), $\text{K}_2\text{CO}_3$ , $\text{H}_2\text{O}$ , reflux, 6 h	96%	89
			Reduction	Aryl halide + aryl boronic acid	Cat. (4 mmol), $\text{K}_2\text{CO}_3$ , PEG-400, 120 °C, 4 h	61–95%	
Herbal tea extract	$\text{Fe}_3\text{O}_4$ @S.	$\text{AgNO}_3$	Reduction	4-Nitrophenol	Cat. (2 mg), $\text{NaBH}_4$ , r.t., 4 min	100%	54
	<i>Lavandulifolia</i> /Ag-NPs	$\text{AgNO}_3$	Suzuki–Miyaura coupling	Aryl halide + phenyl boronic acid	Cat. (0.004 g), $\text{K}_2\text{CO}_3$ , $\text{H}_2\text{O}$ , 60 °C, 1–2 h	70–98%	80
	Ag-NPs@MWCNTs@S.		A <sup>3</sup> -coupling	Aldehydes + amines + alkenes	Cat. (10 mol%), toluene, 100 °C, 8 h	70–96%	141
	<i>lavandulifolia</i> Pd-NPs@S.	PdCl <sub>2</sub>	Suzuki–Miyaura coupling	Aryl halide + phenyl boronic acid	Cat. (2 mg), $\text{K}_2\text{CO}_3$ , EtOH, 100 °C, 0.25–24 h	Traces 99%	87
	<i>Au/S. lavandulifolia</i> NPs	HAuCl <sub>4</sub>	One-pot condensation/ Cyclization	2-Naphthol derivatives	Cat. (50 mL), $\text{H}_2\text{O}_2$ , pH = 5.4, 25 °C, 0.2–96 h	6–47%	95
Yerba Mate	PdISM	PdCl <sub>2</sub>	Denitrogenative C–C coupling (biaryl synthesis)	<i>o</i> -Phenylenediamine/ <i>o</i> -aldehydes	Cat. (10 wt%), EtOH, r.t., 45–65 min	75–94%	103
<i>Camellia sinensis</i>	<i>C. sinensis</i> cell culture	—	Aryl bromides + aryl hydrazines	Cat. (2 mol%), $\text{Na}_2\text{CO}_3$ , EtOH: $\text{H}_2\text{O}$ (1:1), 40 °C, 12 h	82–92%	126	
	MTLAC-SA	—	One-pot three-component condensation (MCR)	Aromatic aldehydes + barbituric acid + ethyl cyanoacetate/Malononitrile	Cat. (5 mol%), EtOH: $\text{H}_2\text{O}$ (1:1), 25 °C, 35–90 min	70–96%	145

isolating key active compounds such as EGCG (epigallocatechin gallate) and theaflavins is crucial to improve reproducibility.

In addition, concerns remain regarding the long-term stability of metal nanoparticles and the potential leaching of metal ions into aqueous media, which could result in negative environmental impacts. This underscores the need for toxicological studies and life cycle assessment (LCA) to ensure the true sustainability and environmental safety of these systems.

Accordingly, the following research directions are suggested for future studies:

- Development of hybrid catalytic systems by combining tea extracts with biobased supports such as biopolymers or MOFs, in order to reach to enhanced catalytic activity and tunability;
- Evaluation of these materials in real-world and industrial applications beyond model reactions like 4-nitrophenol reduction, particularly in pharmaceutical synthesis and wastewater treatment;
- Standardization of tea extracts to reduce performance fluctuations between different catalyst batches.

Moreover, it is essential to emphasize the industrial and environmental significance of tea-based catalysts. Attributes such as easy availability, low cost, green synthesis methods, and renewability make these materials attractive candidates for various industrial applications. However, bridging the gap between laboratory-scale performance and actual industrial implementation will require interdisciplinary collaboration among organic chemistry, materials science, and environmental engineering.

Applications such as industrial wastewater treatment, biomass conversion, green drug synthesis, and removal of organic pollutants from the environment are among the fields where tea-derived catalysts can offer clear benefits. With further optimization, standardization, and validation, these systems have the potential to serve as sustainable and efficient alternatives to traditional, expensive, and toxic catalysts.

In this context, Table 1 represents a comparative overview of different types of tea-derived nanocatalysts. It summarizes key data such as tea type, target reaction, recyclability, main advantages, and reported challenges—providing a clear snapshot of the current landscape in this research field. For readers seeking more detailed information, Table 2 presents a comprehensive summary of the catalysts, including their composition, metal salt, reaction type substrates, reaction conditions, and corresponding yields or conversions in various organic transformations.

## Conclusion

In this article, the synthesis and application of various catalysts derived from different types of teas and herbal infusions have been comprehensively reviewed. The catalysts introduced herein have been thoroughly characterized using a wide range of techniques including FT-IR, UV-Vis, XRD, XPS, SEM, FE-SEM, TEM, BET, TGA/DTG, EDS, EDX, VSM, ICP, ICP-OES, ICP-AES and Boehm titration, confirming their structural, morphological, and surface properties. Tea extracts, rich in polyphenols, flavonoids, alkaloids, and terpenoids, serve as eco-friendly

sources of reducing and stabilizing agents that play a crucial role in the green synthesis of these catalysts.

These bio-derived catalysts have demonstrated significant efficiency in promoting several key organic transformations, such as the reduction of toxic nitrophenol derivatives, the formation of bisphenols *via* Suzuki–Miyaura cross-coupling reactions, and various multicomponent reactions (MCRs), each affording valuable products in high yields and under mild conditions, often within short reaction times.

Notably, most of the investigated catalysts exhibit excellent reusability, maintaining their catalytic activity over multiple reaction cycles with minimal loss in performance. This recyclability, combined with green synthesis routes and the use of renewable plant-based precursors, highlights the potential of tea-derived catalysts as sustainable alternatives in modern green chemistry and industrial applications.

Despite these advances, realizing the full industrial potential of these bio-based catalysts requires continuous development and interdisciplinary collaboration across materials science, environmental engineering, and industrial chemistry. Targeted applications such as wastewater treatment, biomass conversion, and green pharmaceutical synthesis represent promising pilot areas to evaluate the performance and environmental impact of these catalysts on a larger scale. With ongoing optimization and validation, tea-derived catalytic systems could play a pivotal role in replacing toxic and costly metal-based catalysts, marking a critical step toward greener industrial technologies.

## Conflicts of interest

The authors declare that they have no conflict of interest.

## Data availability

No primary research results, software or code have been included and no new data were generated or analysed as part of this article.

## Acknowledgements

The authors are thankful to the University of Guilan Research Council for helping to do this work.

## References

- 1 V. Aggarwal, A. Kachore, E. Bala, H. Singh, M. Selvaraj, M. A. Assiri, R. Kumar, R. Sharma and P. K. Verma, *J. Taiwan Inst. Chem. Eng.*, 2025, **175**, 106249.
- 2 M. Kaur, D. Bharti, P. K. Verma, V. Kumar and R. Kumar, *Int. J. Biol. Macromol.*, 2025, 146389.
- 3 V. Aggarwal, A. Kachore, E. Bala, H. Singh, M. Selvaraj, M. A. Assiri, R. Kumar and P. K. Verma, *J. Phys. Chem. Solids*, 2026, **208**, 113060.
- 4 S. Peta and S. Singh, *Nanoscale*, 2025, **17**, 3708–3713.
- 5 S. Pastoriza, S. Perez-Burillo and J. Á. Rufián-Henares, *Curr. Opin. Food Sci.*, 2017, **14**, 7–12.



6 J. H. Ye, Y. Ye, J. F. Yin, J. Jin, Y. R. Liang, R. Y. Liu, P. Tang and Y. Q. Xu, *Trends Food Sci. Technol.*, 2022, **123**, 130–143.

7 A. Sehgal, *J. S. Afr. Bot.*, 2022, **144**, 92–96.

8 C. J. Etheridge and E. Derbyshire, *Nutr. Food Sci.*, 2020, **50**, 969–985.

9 D. Li, R. Wang, J. Huang, Q. Cai, C. S. Yang, X. Wan and Z. Xie, *Nutrients*, 2019, **11**, 1115.

10 N. Khan and H. Mukhtar, *Nutrients*, 2018, **11**, 39.

11 J. Cao, J. Han, H. Xiao, J. Qiao and M. Han, *Nutrients*, 2016, **8**, 762.

12 L. Zhang, Q. Q. Cao, D. Granato, Y. Q. Xu and C. T. Ho, *Trends Food Sci. Technol.*, 2020, **101**, 139–149.

13 H. Chemingui, A. Moulahi, T. Missaoui, A. H. Al-Marri and A. Hafiane, *Environ. Technol.*, 2024, **45**, 926–944.

14 M. Abdolmaleki, L. Shahsavani and T. Mostaghim, *J. Food Bioprocess Eng.*, 2023, **6**, 81–91.

15 S. Majedi, A. O. Yassen and S. Y. Issa, *Chem. Rev. Lett.*, 2024, **7**, 294–310.

16 F. Coban, H. Ozer, B. Yilmaz and Y. Lan, *Front. Plant Sci.*, 2025, **16**, 1562931.

17 C. I. Heck and E. G. De Mejia, *J. Food Sci.*, 2007, **72**, R138–R151.

18 J. Płatkiewicz, D. Okołowicz, R. Frankowski, T. Grześkowiak, M. Jeszka-Skowron and A. Zgoła-Grześkowiak, *Antioxidants*, 2024, **13**, 1467.

19 M. N. Cha, H. J. Kim, B. G. Kim and J. H. Ahn, *J. Microbiol. Biotechnol.*, 2014, **24**, 1109–1117.

20 M. Nasrollahzadeh, M. Atarod and S. M. Sajadi, *Appl. Surf. Sci.*, 2016, **364**, 636–644.

21 E. Bala, A. Kachore, V. Aggarwal, H. Singh, M. Selvaraj, R. Kumar and P. K. Verma, *Colloids Surf., A*, 2025, **708**, 135961.

22 C. Zhou, D. Deng, C. Huang, Y. Xie, H. Dong, Y. Wen, B. Li, Z. Zhou, W. Luo and Z. Zhou, *J. Anal. Appl. Pyrolysis*, 2024, **177**, 106323.

23 K. Liu, Q. Chen, H. Luo, R. Li, L. Chen, B. Jiang, Z. Liang, T. Wang, Y. Ma and M. Zhao, *Molecules*, 2023, **28**, 1722.

24 M. Nasrollahzadeh and S. M. Sajadi, *J. Colloid Interface Sci.*, 2016, **462**, 243–251.

25 H. Khan, S. Piccolella and S. Pacifico, *Mater. Today Sustain.*, 2025, 101195.

26 H. Singh, A. Kachore, V. Aggarwal, E. Bala, Saima, M. Selvaraj and P. K. Verma, *Chem. Rec.*, 2500069.

27 A. Kachore, E. Bala, V. Aggarwal, H. Singh, M. H. A. Suleiman, M. Selvaraj and P. K. Verma, *J. Ind. Eng. Chem.*, 2025, **146**, 494–505.

28 H. Singh, M. F. Desimone, S. Pandya, S. Jasani, N. George, M. Adnan, A. Aldarhami, A. S. Bazaid and S. A. Alderhami, *Int. J. Nanomed.*, 2023, 4727–4750.

29 P. Panchal, P. Rauwel, S. P. Nehra, P. Singh, M. Karla, G. Hermosa and E. Rauwel, *Pharmaceuticals*, 2025, **18**, 820.

30 R. Thrilokraj, J. G. Małecki, S. Budagumpi, U. A. Kshirsagar and R. B. Dateer, *Green Chem.*, 2024, **26**, 4723–4732.

31 A. Yumni Baharom, A. Norman and C. A. Che Abdullah, *Newsletter, e-Science, Putra*, 2025.

32 S. R. Almisbah, A. M. Mohammed, A. Elgamouz, A. Bihi and A. Kawde, *Water Sci. Technol.*, 2023, **87**, 3059–3071.

33 H. Singh, A. Kachore, V. Aggarwal, E. Bala, Saima, R. Kumar, P. Kumar and P. K. Verma, *ChemistrySelect*, 2025, **10**, e202501004.

34 N. Nishiwaki, *Nitro Compounds and Their Derivatives in Organic Synthesis*, MDPI-Multidisciplinary Digital Publishing Institute, 2020.

35 T. Tamiri and S. Zitrin, 2013, 64–84.

36 M. Ahmed, B. Rappenglueck, L. Ganranoo and P. K. Dasgupta, *Chemosphere*, 2023, **338**, 139499.

37 S. Weihua, Z. Zheng, A. S. Rami, Z. Tao and H. Desheng, *Radiat. Phys. Chem.*, 2002, **65**, 559–563.

38 M. L. Farré, A. Oubiña, M. P. Marco, A. Ginebreda, L. Tirapu and D. Barceló, *Environ. Sci. Technol.*, 1999, **33**, 3898–3904.

39 J. Luan and A. Plaisier, *J. Membr. Sci.*, 2004, **229**, 235–239.

40 J. Zhang, X. Zhao, W. Wang, Y. Mao, J. Sun, Z. Song and P. Zhou, *Colloids Surf., A*, 2023, **678**, 132520.

41 A. Hidalgo, G. León, M. Gómez, M. Murcia, E. Gómez and C. Giner, *J. Water Process Eng.*, 2015, **7**, 169–175.

42 Z. I. Bhatti, H. Toda and K. Furukawa, *Water Res.*, 2002, **36**, 1135–1142.

43 C. Yin, J. Cai, L. Gao, J. Yin and J. Zhou, *J. Hazard. Mater.*, 2016, **305**, 15–20.

44 H. Zhang, C. Fei, D. Zhang and F. Tang, *J. Hazard. Mater.*, 2007, **145**, 227–232.

45 W. Muersha and G. S. P. Soylu, *J. Mol. Struct.*, 2018, **1174**, 96–102.

46 S. Chatterjee, M. Chakraborty, K. K. Bera, A. Mahajan, S. Banik, P. S. Roy and S. K. Bhattacharya, *IOP Conference Series: Materials Science and Engineering*, 2021.

47 G. Varank, A. Demir, K. Yetilmezsoy, S. Top, E. Sekman and M. Sinan Bilgili, *Indian J. Chem. Technol.*, 2012, **19**, 7–25.

48 J. Chen, C. Jin, S. Sun, D. Yang, Y. He, P. Gan, W. G. Nalume, Y. Ma, W. He and G. Li, *Resour. Conserv. Recycl.*, 2023, **198**, 107172.

49 M. Zabihzadeh, F. Shirini, H. Tajik, Z. Shokri and S. Karami, *J. Nanosci. Nanotechnol.*, 2020, **20**, 121–127.

50 Z. Dong, T. Wang, J. Zhao, T. Fu, X. Guo, L. Peng, B. Zhao, N. Xue, W. Ding and Z. Xie, *Appl. Catal., A*, 2016, **520**, 151–156.

51 H. Houcini, F. Laghrib, M. Bakasse, S. Lahrich and M. El Mhammedi, *J. Environ. Anal. Chem.*, 2020, **100**, 1566–1577.

52 W. Raza, in *Sustainable Materials and Green Processing for Energy Conversion*, Elsevier, 2022, pp. 237–261.

53 N. K. Kalita and J. N. Ganguli, *Inorg. Nano-Met. Chem.*, 2017, **47**, 788–793.

54 M. Shahriary, H. Veisi, M. Hekmati and S. Hemmati, *Mater. Sci. Eng., C*, 2018, **90**, 57–66.

55 R. Purbia and S. Paria, *J. Colloid Interface Sci.*, 2018, **511**, 463–473.

56 Y. Bao, J. He, K. Song, J. Guo, X. Zhou and S. Liu, *J. Chem.*, 2021, **2021**, 6562687.

57 B. Kumar, K. Smita, L. Cumbal and A. Debut, *Saudi J. Biol. Sci.*, 2017, **24**, 45–50.

58 M. Nasrollahzadeh, S. M. Sajadi, A. Rostami-Vartooni, M. Alizadeh and M. Bagherzadeh, *J. Colloid Interface Sci.*, 2016, **466**, 360–368.



59 V. Aggarwal, E. Bala, S. Saima, S. Pathan, S. Guleria, S. Sharma, M. Selvaraj and P. K. Verma, *Synlett*, 2024, **35**, 245–267.

60 Z. Wang, C. Xu, X. Li and Z. Liu, *Colloids Surf. A*, 2015, **485**, 102–110.

61 Z. Wang, Y. Huang, D. Lv, G. Jiang, F. Zhang and A. Song, *Green Chem. Lett. Rev.*, 2019, **12**, 197–207.

62 H. Veisi, S. Kazemi, P. Mohammadi, P. Safarimehr and S. Hemmati, *Polyhedron*, 2019, **157**, 232–240.

63 S. Lebaschi, M. Hekmati and H. Veisi, *J. Colloid Interface Sci.*, 2017, **485**, 223–231.

64 K. Mallikarjuna, C. Bathula, K. Buruga, N. K. Shrestha, Y. Y. Noh and H. Kim, *Mater. Lett.*, 2017, **205**, 138–141.

65 H. Veisi and F. Ghorbani, *Appl. Organomet. Chem.*, 2017, **31**, e3711.

66 E. C. Alegria, A. P. Ribeiro, M. Mendes, A. M. Ferraria, A. M. B. d. Rego and A. J. Pombeiro, *Nanomaterials*, 2018, **8**, 320.

67 H. Veisi, A. Rostami and M. Shirinbayan, *Appl. Organomet. Chem.*, 2017, **31**, e3609.

68 S. Paul and J. H. Clark, *Green Chem.*, 2003, **5**, 635–638.

69 M. M. Heravi and E. Hashemi, *Tetrahedron*, 2012, **68**, 9145–9178.

70 M. P. Lati, M. I. Naeem, M. Alinia-Asli, F. Shirini, M. A. Rezvani, B. Åkermark, E. V. Johnston and O. Verho, *ChemistrySelect*, 2018, **3**, 7970–7975.

71 E. B. Mubofu, J. H. Clark and D. J. Macquarrie, *Green Chem.*, 2001, **3**, 23–25.

72 N. Miyaura and A. Suzuki, *Chem. Rev.*, 1995, **95**, 2457–2483.

73 A. Suzuki, *J. Organomet. Chem.*, 1999, **576**, 147–168.

74 N. Miyaura, K. Yamada and A. Suzuki, *Tetrahedron Lett.*, 1979, **20**, 3437–3440.

75 C. P. Delaney, D. P. Marron, A. S. Shved, R. N. Zare, R. M. Waymouth and S. E. Denmark, *J. Am. Chem. Soc.*, 2022, **144**, 4345–4364.

76 A. Ahmed, I. Mushtaq and S. Chinnam, *Futur. J. Pharm. Sci.*, 2023, **9**, 67.

77 M. Farhang, A. R. Akbarzadeh, M. Rabbani and A. M. Ghadiri, *Polyhedron*, 2022, **227**, 116124.

78 H. Targhan, A. Rezaei, A. Aliabadi, A. Ramazani, Z. Zhao and H. Zheng, *Sci. Rep.*, 2024, **14**, 536.

79 I. P. Beletskaya, F. Alonso and V. Tyurin, *Coord. Chem. Rev.*, 2019, **385**, 137–173.

80 H. Veisi, R. Ghorbani-Vaghei, S. Hemmati, M. H. Aliani and T. Ozturk, *Appl. Organomet. Chem.*, 2015, **29**, 26–32.

81 S. S. Gujral, S. Khatri, P. Riyal and V. Gahlot, *Indo Global J. Pharm. Sci.*, 2012, **2**, 351–367.

82 G. Dhangar, J. L. Serrano, C. Schulzke, K. C. Gunturu and A. R. Kapdi, *ACS Omega*, 2017, **2**, 3144–3156.

83 A. Sanzone, A. Calascibetta, M. Monti, S. Mattiello, M. Sassi, F. Corsini, G. Griffini, M. Sommer and L. Beverina, *ACS Macro Lett.*, 2020, **9**, 1167–1171.

84 M. Saleh, M. Baumgarten, A. Mavrinckiy, T. Schäfer and K. Müllen, *Macromolecules*, 2010, **43**, 137–143.

85 R. Chinchilla and C. Nájera, *Chem. Rev.*, 2007, **107**, 874–922.

86 H. Veisi, M. Ghorbani and S. Hemmati, *Mater. Sci. Eng., C*, 2019, **98**, 584–593.

87 C. R. Schmitt, F. A. Duarte, M. Godoi, C. R. Peixoto, F. Trombetta and G. R. Rosa, *SN Appl. Sci.*, 2021, **3**, 243.

88 M. Hekmati, F. Bonyasi, H. Javaheri and S. Hemmati, *Appl. Organomet. Chem.*, 2017, **31**, e3757.

89 C. Bathula, K. Mallikarjuna, D. R. Cuddapah, K. C. Kumar, H.-S. Kim, C. Bai and I. N. Reddy, *Inorg. Chem. Commun.*, 2024, **162**, 112177.

90 G. Bringmann, R. Walter and R. Weirich, *Angew. Chem. Int. Ed. Engl.*, 1990, **29**, 977–991.

91 C. Rosini, L. Franzini, A. Raffaelli and P. Salvadori, *Synthesis*, 1992, 503–517.

92 R. Zimmer, J. Suhrbier and J. Prakt, *Chem. Ztg.*, 1997, **339**, 758–762.

93 Y. Kashiwagi, H. Ono and T. Osa, *Chem. Lett.*, 1993, 257–260.

94 M. Sridhar, S. K. Vadivel and U. T. Bhalerao, *Tetrahedron Lett.*, 1997, **38**, 5695–5696.

95 M. Takemoto, Y. Suzuki and K. Tanaka, *Tetrahedron Lett.*, 2002, **43**, 8499–8501.

96 Z. Wang, R. Xie, H. Hong, L. Han and N. Zhu, *J. CO2 Util.*, 2021, **51**, 101644.

97 G. Kavya, A. R. Nair and A. Sivan, *Mini-Rev. Org. Chem.*, 2023, **20**, 333–357.

98 P. J. Wanjari, N. Saha, G. Dubey and P. V. Bharatam, *Tetrahedron*, 2023, **130**, 133143.

99 F. P. Roudsari, M. Seddighi, F. Shirini and H. Tajik, *Org. Prep. Proced. Int.*, 2020, **52**, 340–353.

100 S. Shojaee and M. Mahdavi Shahri, *Appl. Organomet. Chem.*, 2018, **32**, e3934.

101 R. B. Vlocskó, M. Mishra, A. I. Stoica, L. Gustin and B. Török, *Tetrahedron Green Chem.*, 2024, **3**, 100035.

102 T. T. Nguyen, X. T. T. Nguyen, T. L. H. Nguyen and P. H. Tran, *ACS Omega*, 2019, **4**, 368–373.

103 M. Goswami, M. M. Dutta and P. Phukan, *Res. Chem. Intermed.*, 2018, **44**, 1597–1615.

104 T. Chen, H. Xiong, J. F. Yang, X. L. Zhu, R. Y. Qu and G. F. Yang, *J. Agric. Food Chem.*, 2020, **68**, 9839–9877.

105 M. Mahdavi Shahri, *J. Nanostruct.*, 2019, **9**, 669–678.

106 L. F. Moor, T. R. Vasconcelos, R. da R. Reis, L. S. Pinto and T. M. da Costa, *Mini-Rev. Med. Chem.*, 2021, **21**, 2209–2226.

107 P. Yadav and K. Shah, *Bioorg. Chem.*, 2021, **109**, 104639.

108 G. Kumar, A. Sathe, V. S. Krishna, D. Sriram and S. M. Jachak, *Eur. J. Med. Chem.*, 2018, **157**, 1–13.

109 S. V. Otari, V. V. Shinde, G. Hui, S. K. Patel, V. C. Kalia, I. W. Kim and J. K. Lee, *Ceram. Int.*, 2019, **45**, 5876–5882.

110 R. Dorel, C. P. Grugel and A. M. Haydl, *Angew. Chem. Int. Ed. Engl.*, 2019, **58**, 17118–17129.

111 M. M. Heravi, V. Zadsirjan, M. Malmir and L. Mohammadi, *Monatsh. Chem.*, 2021, **152**, 1127–1171.

112 H. Veisi, T. Tamoradi, B. Karmakar and S. Hemmati, *J. Phys. Chem. Solids*, 2020, **138**, 109256.

113 A. Dhakshinamoorthy, A. M. Asiri and H. Garcia, *ACS Catal.*, 2018, **9**, 1081–1102.

114 H. Veisi, B. Karmakar, T. Tamoradi, S. Hemmati, M. Hekmati and M. Hamelian, *Sci. Rep.*, 2021, **11**, 1983.

115 N. Anbu, N. Nagarjun, M. Jacob, J. M. V. K. Kalaiarasi and A. Dhakshinamoorthy, *Chemistry*, 2019, **1**, 69–79.



116 G. M. Vos, K. C. Hooijssuur, Z. Li, J. Fjeldsted, C. Klein, R. P. de Vries, J. S. Toraño and G. J. Boons, *Nat. Commun.*, 2023, **14**, 6795.

117 N. Seyed, L. Nazemi-Nasymahale, F. Shirini and H. Tajik, *ChemistrySelect*, 2023, **8**, e202204306.

118 M. Wang, W. Zhou, W. Cao, K. Yang, Z. Zhang, X. Zhang and M. Xiong, *Inorg. Chem. Commun.*, 2023, **155**, 111092.

119 M. Simonetti, D. M. Cannas and I. Larrosa, in *Advances in Organometallic Chemistry*, Elsevier, 2017, vol. 67, pp. 299–399.

120 S. Kotha, K. Lahiri and D. Kashinath, *Tetrahedron*, 2002, **58**, 9633–9695.

121 F. W. Forman and I. Sucholeiki, *J. Org. Chem.*, 1995, **60**, 523–528.

122 A. Bhattacharjya, P. Klumphu and B. H. Lipshutz, *Nat. Commun.*, 2015, **6**, 7401.

123 M. Pagliaro, V. Pandarus, R. Ciriminna, F. Béland and P. Demma Carà, *ChemCatChem*, 2012, **4**, 432–445.

124 R. H. Taylor and F. X. Felpin, *Org. Lett.*, 2007, **9**, 2911–2914.

125 P. Das and W. Linert, *Coord. Chem. Rev.*, 2016, **311**, 1–23.

126 S. Hegde and A. Nizam, *Catal. Commun.*, 2024, **187**, 106862.

127 S. Javanshir, N. Saghiran Pourshiri, Z. Dolatkhah and M. Farhadnia, *Monatsh. Chem.*, 2017, **148**, 703–710.

128 S. S. Jin, M. H. Ding and H. Y. Guo, *Heterocycl. Commun.*, 2013, **19**, 139–143.

129 P. Hajiabbasi, G. Mohammadi Ziarani, A. Badiei and A. Abolhasani Soorki, *J. Iran. Chem. Soc.*, 2015, **12**, 57–65.

130 R. S. Ghogare, *Org. Commun.*, 2022, **15**, 44–58.

131 C. Monika, S. Ram and P. K. Sharma, *Asian J. Org. Chem.*, 2023, **12**, e202200616.

132 A. Mohammadi, H. Keshvari, R. Sandaroos, H. Rouhi and Z. Sepehr, *J. Chem. Sci.*, 2012, **124**, 717–722.

133 B. Török, C. Schäfer and A. Kokel, in *Heterogeneous Catalysis in Sustainable Synthesis*, eds. B. Török, C. Schäfer and A. Kokel, Elsevier, 2022, pp. 443–489.

134 N. H. Nasab and J. Safari, *J. Mol. Struct.*, 2019, **1193**, 118–124.

135 P. Mardaneh and A. R. Sardarian, *J. Iran. Chem. Soc.*, 2024, **21**, 211–225.

136 K. Lauder, A. Toscani, N. Scalacci and D. Castagnolo, *Chem. Rev.*, 2017, **117**, 14091–14200.

137 R. Manujyothi, T. Aneja and G. Anilkumar, *RSC Adv.*, 2021, **11**, 19433–19449.

138 T. K. Saha and R. Das, *ChemistrySelect*, 2018, **3**, 147–169.

139 X. Sheng, K. Chen, C. Shi and D. Huang, *Synthesis*, 2020, **52**, 1–20.

140 A. B. Dyatkin and R. A. Rivero, *Tetrahedron Lett.*, 1998, **39**, 3647–3650.

141 H. Veisi, M. Farokhi, M. Hamelian and S. Hemmati, *RSC Adv.*, 2018, **8**, 38186–38195.

142 A. Kumar, K. K. Bhagat, A. K. Singh, H. Singh, T. Angre, A. Verma, H. Khalilullah, M. Jaremko, A. H. Emwas and P. Kumar, *RSC Adv.*, 2023, **13**, 6872–6908.

143 M. M. Surchani, F. Shirini, H. Tajik and O. Goli Jolodar, *Iran. J. Catal.*, 2024, **14**, 142427.

144 M. Amiri, N. Seyed, F. Shirini and H. Tajik, *J. Mol. Struct.*, 2025, **1336**, 141904.

145 L. Dou, X. Zhang, M. M. Zangeneh and Y. Zhang, *Bioorg. Chem.*, 2021, **106**, 104468.

146 C. Wang, B. Karmakar, N. S. Awwad, H. A. Ibrahium, A. F. El-Kott, M. M. Abdel-Daim, A. A. A. Oyouni, O. Al-Amer and G. E. S. Batiha, *Arab. J. Chem.*, 2022, **15**, 103809.

147 N. Daneshvar, O. Goli-Jolodar, R. Karimi-Chayjani, M. S. Nikoo Langarudi and F. Shirini, *ChemistrySelect*, 2019, **4**, 1562–1566.

148 L. Xu, L. Zhang, D. Ren, Y. Peng, Z. Liu, Y. Meng, W. Deng and Y. Zhang, *Inorg. Chem. Commun.*, 2022, **144**, 109927.

149 D. Z. Hou, P. Ling, Y. Zhu, Y. M. Ouyang and B. Karmakar, *Arab. J. Chem.*, 2022, **15**, 104219.

150 Y. Liu, J. Liu, R. Zhang, Y. Guo, H. Wang, Q. Meng, Y. Sun and Z. Liu, *Molecules*, 2019, **24**, 891.

151 M. Khashaei, L. Kafi-Ahmadi, S. Khademinia, A. Poursattar Marjani and E. Nozad, *Sci. Rep.*, 2022, **12**, 8585.

152 X. Ma, S. M. Cooper, F. Yang, W. Hu and H. O. Sintim, *Curr. Org. Chem.*, 2016, **20**, 82–101.

153 A. Dasgupta, E. Richards and R. L. Melen, *ACS Catal.*, 2021, **12**, 442–452.

154 M. A. Garcia, Á. García-Muñoz, J. A. Pena, J. Trujillo-Reyes, R. A. Morales-Luckie, M. Avalos-Borja, A. R. Vilchis-Nestor, V. Sánchez-Mendieta, D. Corona and E. Cuevas-Yañez, *Lett. Org. Chem.*, 2012, **9**, 2.

155 S. Bagheri and N. M. Julkapli, *Int. J. Hydrogen Energy*, 2016, **41**, 14652–14664.

156 Z. Jing, Y. Guo, Q. Wang, X. Yan, G. Yue, Z. Li, H. Liu, R. Qin, C. Zhong and M. Li, *Nat. Commun.*, 2024, **15**, 5806.

157 J. G. de Vries and C. J. Elsevier, *Handbook of Homogeneous Hydrogenation*, WeinheimWiley-VCH, 2007.

158 R. Hudson, G. Hamasaka, T. Osako, Y. M. Yamada, C. J. Li, Y. Uozumi and A. Moores, *Green Chem.*, 2013, **15**, 2141–2148.

159 A. Aires, in *Technologies to Recover Polyphenols from AgroFood By-Products and Wastes*, Elsevier, 2022, pp. 337–357.

160 E. M. Sharshira, A. A. Ataalla, M. Hagar, M. Salah, M. Jaremko and N. Shehata, *Molecules*, 2022, **27**, 5409.

161 B. Kalayci, N. Kaplan, S. Dadi, I. Ocsoy and E. Gokturk, *Polym. Adv. Technol.*, 2024, **35**, e6272.

162 M. A. Garcia, Á. García-Muñoz, J. A. Pena, J. Trujillo-Reyes, R. A. Morales-Luckie, M. Avalos-Borja, A. R. Vilchis-Nestor, V. Sánchez-Mendieta, D. Corona and E. Cuevas-Yañez, *Lett. Org. Chem.*, 2012, **9**, 2–6.

163 C. R. Schmitt, F. A. Duarte, M. Godoi, C. R. Peixoto, F. Trombetta and G. R. Rosa, *SN Appl. Sci.*, 2021, **3**, 1–9.

